Targeting Cbx3/HP1γ Induces LEF-1 and IL-21R to Promote Tumor-Infiltrating CD8 T-Cell Persistence

To-Ha Thai (tthai@bidmc.harvard.edu)
Beth Israel Deaconess Medical Center, Harvard Medical School

Phuong Le
Beth Israel Deaconess Medical Center, Harvard Medical School

Ngoc Ha
Drexel University

Ngan Tran
Beth Israel Deaconess Medical Center, Harvard Medical School

Andrew Newman
Institut für Zell- und Neurobiologie Charité - Universitätsmedizin Berlin

Katharine Esselen
Beth Israel Deaconess Medical Center, Harvard Medical School

John Dalrymple
Beth Israel Deaconess Medical Center Harvard Medical School

Eva Schmelz
Virginia Tech

Avinash Bhandoola
National Cancer Institute https://orcid.org/0000-0002-4657-8372

Hai-Hui Xue
Hackensack University Medical Center https://orcid.org/0000-0002-9163-7669

Prim Singh
Nazarbayev University School of Medicine

Article

Keywords: Cbx3/HP1g, LEF-1, IL-21R or IL-21 receptor, tumor-infiltrating CD8+ T-cell persistence, adoptive T-cell therapy (ACT), effector memory/progenitor memory CD8+ T cells, ovarian cancer, neuroblastoma, melanoma.

Posted Date: March 29th, 2021

DOI: https://doi.org/10.21203/rs.3.rs-343458/v1

Targeting *Cbx3*/HP1γ Induces LEF-1 and IL-21R to Promote Tumor-Infiltrating CD8 T-Cell Persistence

Phuong T. Le[1], Ngoc Ha[1,3], Ngan K. Tran[1,4], Andrew G. Newman[5], Katharine M. Esselen[6], John L. Dalrymple[6], Eva M. Schmelz[7], Avinash Bhandoola[8,11], Hai-Hui Xue[9,11], Prim B. Singh[10,11], and To-Ha Thai[1,2,11,12,*]

[1]Department of Pathology, Beth Israel Deaconess Medical Center, Harvard Medical School, Boston, MA 02115, USA

[2]Cancer Research Institute, Beth Israel Deaconess Medical Center, Harvard Medical School, Boston, MA 02115, USA

[5]Institute of Cell and Neurobiology, Charité-Universitätsmedizin Berlin, Corporate member of Freie Universität Berlin, Humboldt-Universität zu Berlin and Berlin Institute of Health, Berlin, Germany

[6]Division of Gynecologic Oncology, Beth Israel Deaconess Medical Center, Harvard Medical School, Boston, MA 02115, USA

[7]Department of Human Nutrition, Food, and Exercise, Virginia Tech, Blacksburg, VA 24061, USA

[8]Center for Cancer Research, National Cancer Institute, Bethesda, MD 20892-4254, USA

[9]Center for Discovery and Innovation, Hackensack University Medical Center, Nutley, NJ 07110, USA

[10]Nazarbayev University School of Medicine, 5/1 Kerei, Zhanibek Khandar Street, Nur-Sultan Z05K4F4, Kazakhstan

[3]Present address: Department of Neurobiology and Anatomy, College of Medicine, Drexel University, Philadelphia, PA 19129, USA

[4]Present address: Center for Drug Discovery, Department of Pharmaceutical Sciences, Northeastern University, Boston, MA 01225, USA

[11]These authors contributed equally

[12]Lead Contact

[*]Correspondence: tthai@bidmc.harvard.edu (THT)

Abstract

Checkpoint blockade can reverse $CD8^+$ T-cell functional exhaustion, and TCF-1 is essential for this process. However, identifying mechanisms that can prevent functional senescence and potentiate $CD8^+$ T-cell persistence in checkpoint blockade non-responsive tumors remains a challenge. We demonstrate that targeting *Cbx3*/HP1γ causes augmented transcription initiation, chromatin remodeling at *Lef1* and *Il21r* leading to increased transcriptional activity at these loci. Mechanistic studies show LEF-1 and IL-21R are required for *Cbx3*/HP1γ-deficient $CD8^+$ effector T cells to persist resulting in improved control of ovarian cancer, melanoma and neuroblastoma in preclinical models. *Cbx3*/HP1γ-deficient $CD8^+$ T cells enhanced persistence in the TME facilitates remodeling of the chemokine/receptor landscape that ensures their optimal tumor invasion at the expense of $CD4^+$ Tregs. Thus, $CD8^+$ T cells heightened effector function consequent to *Cbx3*/HP1γ deficiency may be distinct from functional reactivation by checkpoint blockade, implicating *Cbx3*/HP1γ as a viable cancer T-cell-based therapy target for resistant, non-responsive solid tumors.

Keywords

Cbx3/HP1γ, LEF-1, IL-21R or IL-21 receptor, tumor-infiltrating $CD8^+$ T-cell persistence, adoptive T-cell therapy (ACT), effector memory/progenitor memory $CD8^+$ T cells, ovarian cancer, neuroblastoma, melanoma.

Introduction

Under persistent antigen exposure as in cancer or chronic infections, $CD8^+$ effector T cells can enter an altered differentiation program known as T-cell exhaustion (T_{EX})[1]. In the tumor microenvironment (TME), $CD8^+$ progenitor T_{EX} cells express unique transcription factors as well as those shared with effector and memory cells including the high mobility group (HMG) transcription factor, T-cell factor 1 (TCF-1, encoded by *Tcf7*). They have reduced effector capacity but can be reinvigorated by check point blockade to proliferate and differentiate into terminally exhausted cells having reduced proliferative capacity yet can efficiently kill tumor cells through perforin 1 (PRF1), granzyme B (GrB) and interferon γ (INFγ)[2, 3, 4]. TCF-1 is implicated in the conversion of $CD8^+$ progenitor T_{EX} to terminally differentiated T_{EX}[5, 6, 7, 8, 9]. However, given that only ~20% of all solid tumors and primarily those harboring high mutation loads respond to checkpoint blockade, in addition to the emergence of checkpoint blockade resistance, there is a

need to identify novel targets that can restore the effector and persistence capacity of exhausted $CD8^+$ T cells in tumors harboring low mutation loads and do not respond to checkpoint blockade. In humans and mice, TCF-1 and the related lymphoid enhancer-binding factor 1 (LEF-1) are functionally linked during T-cell development in the thymus and the generation of precursor and functional memory $CD8^+$ as well as $CD4^+$ T cells[10, 11, 12, 13, 14, 15, 16, 17, 18]. Nevertheless, unlike TCF-1, a role for LEF-1 in tumor response has not been documented.

IL-21R is widely expressed on various innate and adaptive immune cell-lineages including activated $CD8^+$ T, $CD4^+$ T_{FH} and NK cells. During the course of a chronic viral infection or under IL-2-deprived conditions IL-21R signaling is critical for preventing $CD8^+$ T-cell exhaustion[19, 20]. In acute viral infections, IL-21R signaling is essential for the proliferation and survival of activated $CD8^+$ T cells as well as the generation of long-lived memory cells[21, 22, 23]. However, the function of IL-21R signaling in cancer is controversial and not completely understood[24, 25, 26, 27, 28].

Here, we demonstrate that targeting *Cbx3*/HP1γ promotes increased/sustained expression of LEF-1 and IL-21R in $CD8^+$ effector T cells. *Cbx3*/HP1γ deficiency leads to augmented transcription initiation and chromatin remodeling at *Lef1* and *Il21r* resulting in increased transcriptional activity at these loci. Genetic ablation of *Lef1* and *Il21r* in *Cbx3*/HP1γ-deficient mice causes a loss of $CD8^+$ effector T cells accompanied by the reduction of *Ifng*, *Gzmb* and *Prf1* expression leading to uncontrolled growth of ovarian, melanoma and neuroblastoma tumors. By contrast, *Tcf7* deletion does not affect the effector function of *Cbx3*/HP1γ-deficient $CD8^+$ T cells. Our data establish that LEF-1 and IL-21R are required for *Cbx3*/HP1γ-deficient $CD8^+$ T cells to expand, persist and maintain their effector capacity in tumors whereas TCF-1 is insufficient. Our findings together with those of others[29, 30, 31] illustrate the complex mechanisms governing $CD8^+$ T-cell effector differentiation and function within a given TME. They underscore the need for continuing exploration of novel targets that can reverse $CD8^+$ T-cell dysfunction in tumors.

Results

***Cbx3*/HP1γ deficiency modulates LEF-1 and IL-21R expression in $CD8^+$ effector T cells.** Previously we showed that germline deletion of the histone code reader *Cbx3*/HP1γ impairs lymphoid-tissue germinal center (GC) reaction and high-affinity antibody response against a thymus (T)-dependent antigen (Ag) in a $CD8^+$ T-cell-intrinsic manner[32]. *Cbx3*/HP1γ deficiency releases the effector capacity of $CD8^+$ T cells to control tumor growth[33]. However, it is not understood why *Cbx3*/HP1γ-deficient $CD8^+$ effector T cells are not subjected to functional

senescence and can persist in tumors. To ensure that *Cbx3*/HP1γ deletion was restricted to $CD8^+$ T cells, all experiments were performed using the CD8α-Cre strain[34] crossed with our *Cbx3*/HP1γ-floxed mice (resulting animals were *Cbx3*/HP1$\gamma^{fl/+}$ and *Cbx3*/HP1$\gamma^{fl/fl}$; collectively designated as *Cbx3*/HP1γ-deficient). Cre recombinase from this CD8α-Cre strain was active in $CD8^+CD4^-$ T cells not in $CD4^+CD8^-$ or $CD11b^+$ cells (Extended Data Fig. 1a). Conditional ablation of *Cbx3*/HP1γ in $CD8^+$ T cells resulted in a near or complete loss of protein expression and phosphorylation (Extended Data Fig. 1b). To determine mechanisms conferring persistence on *Cbx3*/HP1γ-deficient $CD8^+$ effector T cells, ChIP-Seq data was analyzed (Extended Data Table 1)[33]. In wild-type (wt) differentiated $CD8^+$ T cells, *Cbx3*/HP1γ was bound to the 5' untranslated region (UTR) surrounding transcriptional start sites (TSSs) of *Lef1* (Fig. 1a,b) and *Il21r* (Fig. 1d,e). Western immunoblots showed an induction of LEF-1 expression in differentiated control $CD8^+$ T cells; however, LEF-1 expression was further elevated in *Cbx3*/HP1γ-deficient $CD8^+$ effector T cells (Fig. 1c). The level of LEF-1 detected in control and deficient thymocytes was similar (Extended Data Fig. 1c). In the absence of exogenous IL-21, differentiated *Cbx3*/HP1γ-deficient $CD8^+$ T cells expressed more IL-21R protein and transcript compared to control cells (Fig. 1f-h). There was a steady expansion of *Cbx3*/HP1γ-deficient $CD8^+$IL-$21R^+$ T cells after differentiation while the growth of control cells remained low throughout the differentiation period (Fig. 1f,i). IL-21R was not detected on thymocytes from control or *Cbx3*/HP1γ-deficient mice (Extended Data Fig. 1d). *In vitro*-differentiated *Cbx3*/HP1γ-deficient $CD8^+$ T cells expressed more *Bcl6* and *Tbx21* (T-bet) mRNAs compared to control cells (Extended Data Fig. 1e)[35]. By contrast *Eomes* transcript and protein levels were reduced (Extended Data Fig. 1e,f)[36]. The effector capacity of *Cbx3*/HP1γ-deficient $CD8^+$ T cells was enhanced as evidenced by an upregulation of *Prf1*, *Gzmb* and *Ifng* mRNA expression (Extended Data Fig. 1g). As a result, more cleaved caspase 3 (CC3) was detected in B16 melanoma tumor cells co-cultured with *Cbx3*/HP1γ-deficient $CD8^+$ effector T cells compared to control co-cultures (Extended Data Fig. 1h). *Cbx3*/HP1γ deficiency in $CD4^+$ T cells did not enhance tumor killing. Our results establish that *Cbx3*/HP1γ deficiency induces the sustained increase of LEF-1 and IL-21R in $CD8^+$ effector T cells, which are endowed with an enhanced effector capacity. IL-21R elevated expression likely provides signals mediating *Cbx3*/HP1γ-deficient $CD8^+$ effector T-cell expansion in the absence of exogenous IL-21.

***Cbx3*/HP1γ regulates *Lef1* and *Il21r* transcription initiation and chromatin remodeling.** The rate of gene expression is governed in part by RNA Pol II initiation, elongation and/or chromatin remodeling. Pol II is phosphorylated at serine 5 (Pol II S5) during initiation of transcription while phosphorylation at serine 2 (Pol II S2) generally indicates chromatin remodeling concomitant with transcriptional elongation. To test whether alterations in transcriptional initiation, elongation and/or chromatin remodeling caused increased LEF-1 and IL-21R expression in *Cbx3*/HP1γ-deficient $CD8^+$ effector T cells, ChIP-qPCR experiments were performed using ChIP-tested antibodies specific for Pol II S2 or S5, and H3K9me3. These results revealed augmented levels of Pol II S5 in or around transcription start sites (TSSs) of *Lef1* and *Il21r* loci in *Cbx3*/HP1γ-deficient $CD8^+$ effector T cells compared to control cells (Fig. 2a,b). Similar levels of Pol II S2 density were observed at both loci in control and deficient $CD8^+$ T cells (Fig. 2c,d). The levels of H3K9me3 deposition at *Lef1* locus was unaltered (Fig. 2e). However, there was a general loss of H3K9me3 around the TSS of *Il21r* locus in *Cbx3*/HP1γ-deficient $CD8^+$ effector T cells (Fig. 2f). Thus, genetic deletion of *Cbx3*/HP1γ in $CD8^+$ effector T cells results in enhanced transcription initiation at *Lef1* and *Il21r* loci, with chromatin remodeling activity taking place in an extended region around the TSS of the *Il21r* locus. These changes likely underpinned the increased and sustained transcriptional activity of *Lef1* and *Il21r*.

***Cbx3*/HP1γ-deficient $CD8^+$ effector T cells can persist and cause tumor rejection.** The increased/sustained expression of LEF-1 and IL-21R together with the enhanced effector capacity exhibited by *Cbx3*/HP1γ-deficient $CD8^+$ effector T cells suggest they can persist to control tumor development. Thus, the ability of *Cbx3*/HP1γ-deficient $CD8^+$ T cells to eradicate solid tumors was evaluated using the mouse ID8 or MOSE-L_{TICv} ovarian, B16 melanoma and NB-9464 neuroblastoma (NBL) tumor models. Ovarian and NBL tumors have low mutation rates, no clear defining tumor-associated antigens (TAAs) and are minimally responsive to checkpoint blockade[37, 38, 39]. Accordingly, syngeneic ID8 or MOSE-L_{TICv} ovarian tumor cells were injected intraperitoneally (IP) into control and *Cbx3*/HP1γ-deficient mice. Mice were monitored until abdominal distension was visible, which indicated increased ascites and mirrored metastasis observed in humans. Tumor growth and production of ascites were inhibited in *Cbx3*/HP1γ-deficient mice compared to controls or mice ectopically expressing *Cbx3*/HP1γ driven by the human T-cell-restricted *Cd2* promoter (*Cbx3*/$HP1\gamma^{Tg}$) (Fig. 3a,b and Extended Data Fig. 2a,b). As

a result, *Cbx3*/HP1γ-deficient mice lived longer than controls (Fig. 3c). *Cbx3*/HP1γ-deficient mice were equally effective in reducing B16 melanoma (Fig. 3d) and NB-9464 NBL tumor burden (Fig. 3f), leading to their increased survival rate compared to controls (Fig. 3e,g). On day 120 after ID8 injection, there was an enrichment of $CD8^+NKG2D^+$ effector T cells and a decrease in $CD4^+CD25^+FOXP3^+$ regulatory T cells (Tregs) in ascites from *Cbx3*/HP1γ-deficient mice compared to control or *Cbx3*/$HP1\gamma^{Tg}$ animals (Fig. 3h,i and Extended Data Fig. 2c,d). Similarly, enrichment of $CD8^+NKG2D^+$ effector T cells and decrease in $CD4^+CD25^+FOXP3^+$ Tregs were observed in B16 melanoma as well as NBL tumors (Fig. 3j-m and Extended Data Fig. 2e-h). To show that *Cbx3*/HP1γ-deficient $CD8^+$ effector T cells alone can persist and cause tumor rejection, $CD8^+$ T cells ($CD45.2^+$) were differentiated *in vitro*. On day 5 after differentiation, $CD8^+$ T cells were collected for adoptive T-cell therapy in tumor bearing congenic B6.SJL ($CD45.1^+$) recipients (Extended Data Fig. 3a). Treatment with *Cbx3*/HP1γ-deficient $CD8^+$ effector T cells alone resulted in a statistically significant decrease in B16 melanoma and NBL tumor burden compared to treatment with control cells (Extended Data Fig. 3b,c). Within B16 melanoma tumors, there was an exclusive enrichment of transferred *Cbx3*/HP1γ-deficient $CD8^+NKG2D^+$ effector T cells, not endogenous nor control *Cbx3*/HP1γ-sufficient $CD8^+$ effector T cells (Extended Data Fig. 3d). Contaminating donor $CD4^+NKG2D^+$ and $NK1.1^+NKG2D^+$ T cells were not detected in tumors or spleens indicating that they were not the source of tumor killing (Extended Data Fig. 3e-h). Inhibition of *Cbx3*/HP1γ-deficient $CD8^+$ effector T cells engagement with tumor cells using a blocking/non-depleting anti-NKG2D antibody resulted in uncontrolled tumor growth and decreased survival of treated animals (Extended Data Fig. 4a-d), accompanied by the reduction of $CD8^+NKG2D^+$ effector T cells in tumors, to a level similar to that of untreated control mice (Extended Data Fig. 4e,f). NKG2D blockade did not affect $CD4^+NKG2D^+$ and $NK1.1^+NKG2D^+$ T-cell frequencies (Extended Data Fig. 4g,h). Comparable frequencies of $NK1.1^+NKG2D^+$ or $CD4^+NKG2D^+$ T cells was recovered from tumors of control, *Cbx3*/$HP1\gamma^{Tg}$ and *Cbx3*/HP1γ-deficient mice (Extended Data Fig. 5). Expression of *Ifng*, *Gzmb* and *Prf1* was elevated in B16 melanoma and NBL tumors excised from *Cbx3*/HP1γ-deficient mice compared to controls or *Cbx3*/$HP1\gamma^{Tg}$ animals (Extended Data Fig. 6a-f). TUNEL staining revealed more apoptotic tumor cells (brown) in melanoma and NBL tumors from *Cbx3*/HP1γ-deficient mice compared to controls (Fig. 3n,o). Genetic ablation of *Prf1* in *Cbx3*/HP1γ-deficient animals led to uncontrolled B16

melanoma growth and decreased tumor-cell apoptosis while *Ifng* deletion resulted in unchecked NBL tumor development in *Cbx3*/HP1γ-deficient mice (Extended Data Fig. 6g-i). Together, our results demonstrate that *Cbx3*/HP1γ-deficient $CD8^+$ effector T cells expressing NKG2D can persist and cause tumor rejection, irrespective of tumor mutation status. The engagement of NKG2D with its ligands expressed on tumor cells likely facilitates the tumor killing activity of *Cbx3*/HP1γ-deficient $CD8^+$ effector T cells through the enhanced production of PRF1, GrB and INF-γ.

***Cbx3*/HP1γ-deficient $CD8^+$ T cells remodel the tumor chemokine/receptor landscape.** $CD8^+$ effector T cells homing to tumors is mediated primarily by the interaction between CCL2/CCR2 and CXCL9/CXCL10/CXCR3 chemokine/receptor pairs while $CD4^+$ Tregs trafficking to tumors is induced mostly by CCL28/CCR10 and CXCL12/CXCR4[40, 41, 42, 43, 44]. Chemokines are generally produced by tumor-associated myeloid cells including dendritic cells (DCs) and macrophages (MØs) whereas their cognate receptors are expressed on T cells as well as other immune cells. It is proposed that changes in the tumor chemokine/receptor landscape influence anti-tumor responses; however, precise mechanisms through which this occurs has not been clearly established. RT-qPCR assays demonstrated that *Ccl2*/*Ccr2* and *Cxcl9/Cxcl10*/*Cxcr3* levels were higher in B16 melanoma tumors from *Cbx3*/HP1γ-deficient mice than those from controls (Fig. 4a,b). In NBL tumors from *Cbx3*/HP1γ-deficient mice, *Ccl2*/*Ccr2* and *Cxl10* remained similar to those of controls whereas *Cxcl9*/*Cxcr3* levels were elevated (Fig. 4c,d). Compared to tumors from controls, *Ccr10* and *Cxcl12*/*Cxcr4* levels were decreased in B16 melanoma tumors from *Cbx3*/HP1γ-deficient mice (Fig. 4e,f). In NBL tumors from *Cbx3*/HP1γ-deficient mice, the level of *Ccl28/Ccr10* and *Cxcl12* expression was reduced (Fig. 4g,h). These observations indicate that homing of *Cbx3*/HP1γ-deficient $CD8^+$ effector T cells into B16 melanoma tumors requires CCL2 and CXCL9/CXCL10 present in the TME and their receptors CCR2 and CXCR3 expressed on $CD8^+$ T cells. However, *Cbx3*/HP1γ-deficient $CD8^+$ effector T cells likely depend on CXCL9/CXCR3 interaction to invade NBL tumors. Changes in the levels of $CD4^+$ Tregs chemokines and receptors suggest that CCR10 and CXCL12/CXCR4 regulate homing of $CD4^+$ Tregs into B16 melanoma tumors while invasion of NBL tumors by $CD4^+$ Tregs is governed by CCL28/CCR10 and CXCL12. In short, the presence of *Cbx3*/HP1γ-deficient $CD8^+$ effector T cells in the TME mediates remodeling of the chemokine/receptor landscape that favors their optimal trafficking into tumors at the expense of $CD4^+$ Tregs.

LEF-1 and IL-21R are indispensable for halting tumor growth. To establish that LEF-1 and IL-21R contribute to the control of tumor growth by *Cbx3*/HP1γ-deficient $CD8^+$ effector T cells, compound mutant mice were created (Extended Data Fig. 7a). In the *Cbx3-Lef1*-deficient mouse, *Lef1* and *Cbx3*/HP1γ deletion was restricted to $CD8^+$ T cells; in the *Cbx3-Il21r*-deficient mouse, *Cbx3*/HP1γ ablation was restricted to $CD8^+$ T cells while *Il21r* was deleted in all tissues. LEF-1 and IL-21R expression was abolished in deficient $CD8^+$ T cells compared to control cells (Fig. 5a,b). Loss of one *Lef1* or *Il21r* allele showed a decrease in protein levels that were almost completely abrogated upon deletion of both alleles. Progenitor T-cell development proceeded normally in the thymus of compound mutant animals (Extended Data Fig. 7b,c). Mesenteric lymph nodes (mLNs) of compound mutant mice displayed normal frequencies of mature $CD8^+$ and $CD4^+$ T cells (Extended Data Fig. 7d,e). Normal ratios of naïve ($CD44^-CD62L^+$), effector ($CD44^+CD62L^-$) and memory ($CD44^+CD62L^+$) T cells were observed in the mLNs of compound mutant animals (Extended Data Fig. 7f,g). In the mLNs, IL-21R expression was restricted to the $CD8^+$ effector ($CD44^+CD62L^-$) T-cell population and was also dependent on gene dosage (Extended Data Fig. 7h). IL-21R was not detected on any $CD4^+$ T-cell populations (Extended Data Fig. 7i). To determine LEF-1 contribution to tumor control, ID8 (ovarian), B16 (melanoma) or NB-9464 (NBL) tumor cells were injected into *Cbx3-Lef1*-deficient and control mice. *Lef1* genetic ablation resulted in unrestrained ovarian, melanoma and NBL tumor growth (Fig. 5c,d,f). Tumor burden was higher than that observed for *Cbx3*/HP1γ-deficient mice, but similar to controls. Because *Il21r* was deleted in all tissues, adoptive transfer of differentiated $CD8^+$ T cells from *Cbx3-Il21r*-deficient and control mice was performed. Melanoma and NBL growth proceeded unchecked in tumor-bearing B6.SJL ($CD45.1^+$) congenic mice treated with control or *Cbx3-Il21r*-deficient $CD8^+$ effector T cells ($CD45.2^+$) compared to animals receiving *Cbx3*/HP1γ-deficient $CD8^+$ effector T cells ($CD45.2^+$) (Fig. 5e,g). Our results showing that *Cbx3-Lef1*-deficient mice cannot control tumor growth indicates that TCF-1, which is intact in our models, may not be sufficient in restraining tumor development. To assess TCF-1 role in tumor control in our model, we created *Cbx3-Tcf7*-deficient mice in which both genes were conditionally abrogated in $CD8^+$ T cells (Extended Data Fig. 8a). Unlike *Lef1* and *Il21r*, deletion of both *Tcf7* alleles was necessary to achieve near complete abrogation of TCF-1 expression (Fig. 5h). Growth of all three tumors was halted in *Cbx3-Tcf7*- and *Cbx3*/HP1γ-deficient mice compared to controls (Fig. 5i-k), *Cbx3-Lef1*-deficient mice or those receiving *Cbx3-Il21r*-deficient $CD8^+$ effector T cells (Fig. 5c-g). Our

data establish that LEF-1 and IL-21R are required for the optimal control of ovarian, melanoma and NBL tumor growth consequent to *Cbx3*/HP1γ deficiency while TCF-1 is insufficient. Moreover, LEF-1 expression in control $CD8^+$ effector T cells is induced (Fig. 1c), yet they are incapable of persisting in tumors, suggesting there may be a threshold of expression level required for LEF-1 to function effectively. IL-21R expression is confined to the $CD8^+$ effector population and its loss following deletion suggest that IL-21R function is essential to this population, which is critical for halting tumor development.

LEF-1 and IL-21R are required for *Cbx3*/HP1γ-deficient $CD8^+$ effector T cells to persist in tumors. The inability of *Cbx3-Lef1*- and *Cbx3-Il21r*-deficient mice to halt tumor development suggests that LEF-1 and IL-21R are required for the persistence of $CD8^+$ effector T cells in tumors. Analyses of tumors from *Cbx3-Lef1*-deficient mice and those receiving *Cbx3-Il21r*-deficient $CD8^+$ T cells (hereafter simplified as *Cbx3-Il21r*-deficient) revealed that the frequency of $CD8^+$ effector T cells was reduced to control levels in all tumors (Fig. 6a-e). By contrast, tumors from *Cbx3-Tcf7*- and *Cbx3*/HP1γ-deficient animals exhibited similar $CD8^+$ effector T-cell frequencies that were elevated over control mice (Fig. 6f-h). The proportion of $CD8^+$ T cells exhibiting progenitor ($CD8^+TIM3^+CXCR5^+$) or terminal exhausted ($CD8^+TIM3^+CXCR5^-$) phenotype was not perturbed (Extended Data Fig. 8b). The frequency of $NK1.1^+NKG2D^+$ and $CD4^+NKG2D^+$ T cells in all tumor types was low and similar to that of controls (Extended Data Fig. 8c). Myeloid and B-cell populations were not altered. Our data underscore the fact that LEF-1 and IL-21R are required for the persistence of *Cbx3*/HP1γ-deficient $CD8^+$ effector T cells in tumors with varied mutation loads and are checkpoint blockade responsive (B16 melanoma) or non-responsive (ovarian and NBL). In the absence of checkpoint blockade, TCF-1 is not sufficient in conferring persistence on $CD8^+$ effector T cells.

LEF-1 and IL-21R are required to maintain effector activity in tumors. To confirm that the loss of $CD8^+$ effector T cells will lead to diminished effector activity in tumors from *Cbx3-Lef1*- and *Cbx3-Il21r*-deficient mice, RT-qPCR assays were done using tumor RNA samples from mutant and control mice. In melanoma tumors from *Cbx3-Lef1*- and *Cbx3-Il21r*-deficient mice, *Prf1* and *Gzmb* transcript levels were reduced to controls, which were lower than those in tumors from *Cbx3*/HP1γ-deficient mice (Fig. 7a-d). *Prf1*, *Gzmb* and *Ifng* expression in NBL tumors from *Cbx3-Lef1*- and *Cbx3-Il21r*-deficient mice was diminished compared to *Cbx3*/HP1γ-deficient mice but similar to that of controls (Fig. 7e-j). By contrast, *Prf1*, *Gzmb* or *Ifng* transcripts were readily

detected in B16 and NBL tumors from *Cbx3*/HP1γ- and *Cbx3-Tcf7*-deficient mice (Fig. 7a,b and e-g). Thus, our findings show that LEF-1 and IL-21R, not TCF-1, are indispensable for maintaining *Prf1*, *Gzmb* and *Ifng* presence in tumors. The loss of $CD8^+$ effector T cells likely contributes to the observed blunted effector activity observed in tumors from *Cbx3-Lef1*- and *Cbx3-Il21r*-deficient mice that in turn results in unchecked tumor growth.

Discussion

We establish that depletion of *Cbx3*/HP1γ in $CD8^+$ T cells simultaneously induces the elevated, sustained expression of factors conferring both persistence and heightened effector capacity on *Cbx3*/HP1γ-deficient $CD8^+$ T cells that in turn enables them to control the growth of diverse tumor types irrespective of mutation loads. Once in the TME, *Cbx3*/HP1γ-deficient $CD8^+$ T cells can remodel the chemokine/receptor landscape that favors their optimal trafficking into tumors at the expense of $CD4^+$ Tregs thus eliminating immune suppression. *Cbx3*/HP1γ deficiency allows for a higher rate of transcription initiation and chromatin remodeling at *Lef1* and *Il21r* loci. Consequently, *Cbx3*/HP1γ-deficient $CD8^+$ T cells express elevated levels of LEF-1 and IL-21R that halt functional senescence and enable their persistence in tumors without the assistance of checkpoint blockade. By contrast, *Tcf7* deletion does not affect the effector function of *Cbx3*/HP1γ-deficient $CD8^+$ T cells. Thus, $CD8^+$ T cells heightened effector function consequent to *Cbx3*/HP1γ deficiency may be distinct to functional reactivation by checkpoint blockade, implicating *Cbx3*/HP1γ as a viable cancer T-cell-based therapy target for resistant, non-responsive solid tumors.

To date, no essential functions for LEF-1 have been identified in $CD8^+$ effector T cells despite *Lef1* expression being detected in human and mouse stem-like tumor infiltrating lymphocyte (TIL) subsets that also express *Tcf7*[7, 9, 29, 45, 46]. Here, we present compelling evidence that LEF-1 has a critical and non-redundant function in tumor rejection. The exclusive increase of *Cbx3*/HP1γ-deficient $CD8^+$ effector T cells in tumors and their subsequent disappearance when *Lef1* is ablated suggest that LEF-1 is required for the persistence of *Cbx3*/HP1γ-deficient $CD8^+$ effector T cells in varied tumor types. Our results showing tumor growth is successfully inhibited in *Cbx3-Tcf7*-deficient mice indicates that TCF-1 function may be insufficient. Our data are distinct to those found with checkpoint blockade where TCF-1 activity is implicated in the rejuvenation of tumor $CD8^+$ T_{EX} cells. Instead, our findings are consistent with those reported by Carr et. al. wherein

they show LEF-1 playing primary roles in the post selection and effector fate differentiation of iNKT2 cells in the thymus[47]. Similarly, Reya and colleagues have shown that LEF-1 is required for progenitor B-cell proliferation and survival through Wnt signaling[48]. In both models, LEF-1 exhibits a more dominant role whereas TCF-1 is not sufficient for the differentiation and expansion of the immune-cell populations examined. Thus, there may be specific conditions wherein LEF-1 function is dominant and sufficient for the development and differentiation of various immune cells while that of TCF-1 is not required.

Our observations that IL-21R$^+$CD8$^+$ effector T cells increase in number after differentiation and are lost upon *Il21r* deletion indicate that IL-21R provides survival as well as expansion signals to these cells. This is in keeping with work showing that, in humans and mice, IL-21R has an essential role in regulating viral infections and tumor immunity. During the course of a chronic viral infection or under IL-2-deprived conditions, IL-21R signaling is critical for preventing CD8$^+$ T-cell exhaustion[19, 20]. In acute viral infections, IL-21R signaling is essential for the proliferation and survival of activated CD8$^+$ T cells as well as the generation of long-lived memory cells[21, 22, 23]. In these models, IL-21R can activate the STAT1/STAT3 signaling pathways, which subsequently upregulate pro-survival factors BCL-2 and BCL-X_L and downregulate TRAIL[22, 23]. Moreover, several lines of evidence indicate that IL-21R is involved in tumor immunity. First, high expression of IL-21R on CD8$^+$ T cells in tumors correlates positively with overall survival and lack of tumor recurrence in hepatocellular carcinoma (HCC) patients[24]. Second, in mice, IL-21R signaling reduces accumulation of myeloid derived suppressor cells (MDSCs) in the TME to control rapid HCC growth and maintains an immunological memory response to tumor re-challenge[24]. Third, newly diagnosed HER2$^+$ breast cancer patients with higher *Il21r* expression may have a reduced risk of distant relapse when treated with trastuzumab (anti-HER2/ErB2 mAb) in combination with chemotherapy; IL-21R expression on CD8$^+$ effector T cells, not NK cells, is required for optimal anti-ErB2 mAb efficacy[25]. Our results underscore IL-21R critical function in providing signals that induce the expansion of CD8$^+$ effector T cells to promote their anti-tumor capacity.

Our results suggest a model whereby *Cbx3*/HP1γ normally restrains the effector and persistence potential of CD8$^+$ T cells, which will eventually succumb to functional inactivation and apoptosis. Removal of the *Cbx3*/HP1γ restraint allows CD8$^+$ T cells to differentiate into long-lived effector cells armed with an intrinsic, heightened killing and persistence capacity to control tumor growth; LEF-1 and IL-21R are required while TCF-1 is insufficient. Our model does not preclude the

possibility that LEF-1 and IL-21R may also be implicated in $CD8^+$ T-cell responses downstream of checkpoint blockade. Since mouse and human *Cbx3*/HP1γ peptides are 100% identical, we suspect that human *Cbx3*/HP1γ will behave identically to the mouse ortholog: *Cbx3*/HP1γ deficiency would have the same effects on human $CD8^+$ T cells. Furthermore, ovarian and neuroblastoma are tumors with low mutation rates that do not respond to checkpoint blockade, yet their growth is effectively controlled by *Cbx3*/HP1γ-deficient $CD8^+$ effector T cells. Thus, our findings provide a rationale for targeting *Cbx3*/HP1γ in human T cells to treat tumors harboring low mutation loads and do not respond to checkpoint inhibitors.

Acknowledgments

We thank the Animal Technicians at the BIDMC Animal Research Facility for their dedication to and diligence in keeping our mouse colonies healthy. We are grateful to Drs. Crystal L. MacKall (Stanford University) and Katherine F. Roby (University of Kansas Medical Center) for the NB-9464 and ID8 tumor cell lines, respectively. We thank Dr. Dimitris Kioussis (MRC/National Institute for Medical Research, UK) for providing the VA-hCD2 vector. We are indebted to Dr. Lina Du at the Dana-Farber/Harvard Cancer Center (DF/HCC) Transgenic Mouse Core for her expertise in generating the *Cbx3*/HP1γ^{Tg} mouse. This work was supported by grants to THT: NIH AI099012, CA198263, Friends for Life Neuroblastoma Research Program and The Mayer Family Fund.

Author Contributions

T.H.T. N.H. and P.T.L. conceived the project and wrote the original draft with input and guidance from K.M.E., J.L.D., E.M.S., A.B., H.H.X., P.B.S.. T.H.T., P.T.L., N.H. and N.K.T. designed and performed experiments. P.T.L., N.H., A.B., H.H.X., P.B.S. and T.H.T. analyzed data and wrote the final manuscript.

Declaration of Interests

The authors declare no competing interests.

Figure Legends

Figure 1. *Cbx3*/HP1γ deficiency modulates LEF-1 and IL-21R expression in $CD8^+$ effector T cells. a, Schematic of mouse *Lef1* locus. -2 and 12 indicated positions of first and last primer pairs, respectively. **b**, Read-density tracks of *Cbx3*/HP1γ peaks across *Lef1* identified by ChIP-Seq using chromatin from wt day 5 differentiated $CD8^+$ T cells (as in **c**, pooled from 3 mice); y axis: number of reads per million mapped per 25-bp window. **c**, LEF-1 expression was assessed by Western

immunoblot using total lysates from differentiated control and *Cbx3*/HP1γ-deficient $CD8^+$ T cells; 3/28+IL2: $CD8^+$ T cells differentiated for 5 days with plate-bound anti-CD3 and anti-CD28 plus IL-2; C: control (CD8α-Cre or wt); fl/+: $Cbx3^{fl/+}$; fl/fl: $Cbx3^{fl/fl}$: $CD8^+$ T-cell-restricted deletion of *Cbx3*/HP1γ using the CD8α-Cre mouse. **d**, Schematic of mouse *Il21r* locus. -4 and 4: positions of first and last pair of primers, respectively. **e**, Read-density tracks of *Cbx3*/HP1γ peaks across *Il21r* identified by ChIP-Seq as in (**b**). **f**, IL-21R expression on differentiated $CD8^+$ T cells was determined by flow cytometry; left panels depicted percent $CD8^+$IL-$21R^+$ cells from each culture; right panels indicated IL-21R levels on the same cells; numbers: percent cells; representative of 3 experiments; n = 3 for each genotype. **g**, Graphs represented IL-21R mean fluorescence intensity (MFI) from (**f**). **h**, Relative expression of *Il21r*, normalized to *Gapdh*, in day 5 differentiated $CD8^+$ T cells was evaluated by RT-qPCR using RNA from cells obtained in (**f**); Graphpad unpaired student t-test: **p≤0.01; representative of 3 experiments. **i**, Number of $CD8^+$IL-$21R^+$ T cells in cultures were calculated from (**f**); Graphpad unpaired student t-test: *p≤0.05, **p≤0.01.

Figure 2. *Cbx3*/HP1γ regulates *Lef1* and *Il21r* transcription initiation and chromatin remodeling. a,**b**, Levels of Pol II S5 bound to *Lef1* (**a**) and *Il21r* (**b**) were quantified by ChIP-qPCR using chromatin from day 5 differentiated $CD8^+$ T cells. TSS: transcription start site, numbers on X axis: positions of primers along the two loci; 150 bp products amplified by *Lef1* or *Il21r* primers. **c**,**d**, Levels of Pol II S2 bound to *Lef1* (**c**) and *Il21r* (**d**) were quantified as in (**a**,**b**). **e**,**f**, H3K9me3 deposition on *Lef1* (**e**) and *Il21r* (**f**) was quantified as in (**a**,**b**). Statistics: Graphpad unpaired student t-test: *p≤0.05, **p≤0.01, ***p≤0.001, ****p≤0.0001; representative of 4 independent ChIPs using pooled chromatin from 3 mice.

Figure 3. *Cbx3*/HP1γ-deficient $CD8^+$ effector T cells can persist and cause tumor rejection. **a**, Ascites from control (CD8α-Cre or wt), $Cbx3^{Tg}$, $Cbx3^{fl/+}$ and $Cbx3^{fl/fl}$ mice (X axis) were visualized on day 120 after intraperitoneal injection of mouse ID8 ovarian tumor cells; $Cbx3^{Tg}$: *Cbx3*/HP1γ T-cell-restricted expression driven by the human *Cd2* promoter; $Cbx3^{fl/+}$ and $Cbx3^{fl/fl}$: $CD8^+$ T-cell-restricted deletion of *Cbx3*/HP1γ using the CD8α-Cre mouse. **b**, Ovarian ascites (vol: volume) of mice in (**a**) were measured and graphed; bars: group median; Graphpad unpaired student t-test: **p≤0.01, ***p≤0.001; each symbol = one mouse; n = 5-8. **c**, Survival curves of ovarian tumor-bearing mice were determined; Graphpad log-rank (Mantel-Cox) test; n = 5-8. **d**, B16 tumor cells were injected subcutaneously (sc) and growth was assessed starting on day 14

after tumor-cell injection then every 2 days through day 20; Graphpad two-way ANOVA: **p≤0.01, ****p≤0.0001; n = 5. **e**, Survival curves of B16 melanoma tumor-bearing mice.; Graphpad log-rank (Mantel-Cox) test; n = 5. **f**, NB-9464 tumor cells were injected sc, NBL tumor growth was determined every 2 days starting on day 22 through day 28; Graphpad two-way ANOVA: ****p≤0.0001; n = 5. **g**, Survival curves of NBL tumor-bearing mice; Graphpad log-rank (Mantel-Cox) test, n = 5. **h**,**j**,**l**, Frequencies of $CD8^+NKG2D^+$ T cells in ovarian ascites, B16 and NBL tumors from control (CD8α-Cre or wt), $Cbx3^{Tg}$, $Cbx3^{fl/+}$ and $Cbx3^{fl/fl}$ mice; data were extracted from flow analysis (Extended Data Fig. 2c,e,g); bars: group median; Graphpad unpaired student t-test: **p≤0.01, ***p≤0.001, ****p≤0.0001; each symbol = one mouse; n = 5-8. **j**,**k**,**m**, Frequencies of $CD4^+FOXP3^+$ Tregs in ovarian ascites, B16 and NBL tumors (Extended Data Fig. 2d,f,h); bars: group median; Graphpad unpaired student t-test: *p≤0.05, **p≤0.01, ***p≤0.001, ****p≤0.0001; each symbol = one mouse; n = 5-8 for each genotype. **n**,**o**, Apoptotic cells (brown) in B16 melanoma and NBL tumor sections were identified by TUNEL staining; representative of 4 tumors from each mouse strain.

Figure 4. *Cbx3*/HP1γ-deficient $CD8^+$ T cells remodel the tumor chemokine/receptor landscape. a,**b**, Relative expression of chemokines and receptors mediating $CD8^+$ T cells trafficking into B16 tumors were measured by RT-qPCR using RNA of day 5 differentiated $CD8^+$ T cells from control and *Cbx3*/HP1γ-deficient $CD8^+$ T cells as in figure 1**c**, results were normalized to *Gapdh*. **c**,**d**, Relative expression of chemokines and receptors mediating $CD8^+$ T cells trafficking into NBL tumors. **e**,**f**, Relative expression of chemokines and receptors inducing $CD4^+$ Tregs homing into B16 tumors normalized to *Gapdh*. **g**,**h**, Relative expression of chemokines and receptors inducing $CD4^+$ Tregs homing into NBL tumors. X axis: mouse strains; Graphpad unpaired student t-test: *p≤0.05, **p≤0.01, ***p≤0.001; ns: not significant; n = 4 tumors from each mouse strain.

Figure 5. LEF-1 and IL-21R are indispensable for halting tumor growth. a, Western blot of LEF-1 expression was done using total lysates of day 5 differentiated $CD8^+$ T cells; C: *Cbx3*/HP1γ-deficient; $Lef1^{fl/+}$ and $Lef1^{fl/fl}$: *Cbx3-Lef1*-deficient. **b**, IL-21R expression was evaluated by flow; $Cbx3^{fl/fl}$: *Cbx3*/HP1γ-deficient; $Il21r^{+/-}$ and $Il21r^{-/-}$: *Cbx3-Il21r*-deficient. **c**, Ovarian ascites were measured on day 125 after tumor injection; bars: group median; Graphpad unpaired student t-test: ***p≤0.001, ****p≤0.0001; each symbol = one mouse; n = 3-5. $Cbx3^{fl/fl}Lef1^{fl/fl}$: *Cbx3-Lef1*-

deficient. **d**, B16 melanoma tumor burden was determined on day 18 after tumor injection; bars: group median; Graphpad unpaired student t-test: ****p≤0.0001; each symbol = mouse; for each genotype n = 4-7. **e**, On day 10 after injection of tumor cells, tumor bearing B6SJ/L mice were treated with *in vitro*-differentiated CD8$^+$ T cells from control, *Cbx3*$^{fl/f}$ or *Cbx3*$^{fl/f}$,*Il21r*$^{-/-}$ (*Cbx3-Il21r*-deficient); ***p≤0.001, n = 3-4 recipients. **f**, NBL tumor burden was determined starting on day 25 after injection of tumor cells then every 2 days until day 33; Graphpad two-way ANOVA: ***p≤0.001; n = 2-5. **g**, On day 14 after NBL injection, tumor bearing B6SJ/L mice were treated with *in vitro*-differentiated CD8$^+$ T cells from control, *Cbx3*$^{fl/f}$ or *Cbx3*$^{fl/f}$,*Il21r*$^{-/-}$ (*Cbx3-Il21r*-deficient); ****p≤0.0001, n = 3-4 recipients. **h**, Western blot of TCF-1 expression was done using total lysates of day 5 differentiated CD8$^+$ T cells; C: *Cbx3*/HP1γ-deficient; *Tcf7*$^{fl/+}$ and *Tcf7*$^{fl/fl}$: *Cbx3-Tcf7*-deficient. **i-k**, Ovarian ascites (**i**), B16 tumor size (**j**) and NBL tumor volume (**k**) were measured in control, *Cbx3*/HP1γ-deficient and *Cbx3-Tcf7*-deficient mice; Graphpad unpaired student t-test: *p≤0.05, **p≤0.01, ***p≤0.001; n = 3-4 per genotype.

Figure 6. LEF-1 and IL-21R are required for *Cbx3*/HP1γ-deficient CD8$^+$ effector T cells to persist in tumors. a,**b**,**c**, Frequencies of CD8$^+$NKG2D$^+$ T cells in ovarian ascites (**a**), B16 (**b**) and NBL (**c**) tumors were determined using data extracted from flow analysis. **d**,**e**, Frequencies of CD8$^+$NKG2D$^+$ T cells (gated on CD45.2$^+$ populations) in B16 melanoma (**d**) and NBL (**e**) tumors from B6.SJL mice treated with *in vitro*-differentiated control, *Cbx3*/HP1γ- or *Cbx3-Lef1*-deficient CD8$^+$ effector T cells on day 10 and day 14 after injection of B16 and NBL tumor cells, respectively. **f-h**, ovarian ascites (**f**), B16 tumor size (**g**) and NBL tumor volume (**h**) of control, *Cbx3*/HP1γ- or *Cbx3-Tcf7*-deficient mice. Statistics: bars: group median; Graphpad unpaired student t-test: *p≤0.05, **p≤0.01, ***p≤0.001, ****p≤0.0001; each symbol = one mouse; n = 3-5.

Figure 7. LEF-1 and IL-21R are required to maintain effector activity in tumors. a,**b**, *Prf*1 and *Gzmb* relative expression in day 18 B16 melanoma tumors was quantified by RT-qPCR using tumor RNA from indicated mice. **c**,**d**, *Prf*1 and *Gzmb* relative expression in day 18 B16 melanoma tumors from B6.SJL mice treated with *in vitro*-differentiated control, *Cbx3*/HP1γ- or *Cbx3-Lef1*-deficient CD8$^+$ effector T cells on day 10 after injection of B16 tumor cells. **e-g**, *Prf1*, *Gzmb* and *Ifng* relative expression in day 33 NBL tumors. **h-j**, *Prf1*, *Gzmb* and *Ifng* relative expression in day 33 NBL tumors from B6.SJL mice treated with *in vitro*-differentiated control, *Cbx3*/HP1γ- or

Cbx3-Lef1-deficient $CD8^+$ effector T cells on day 14 after injection of NBL tumor cells. Statistics: Graphpad unpaired student t-test: *p≤0.05, **p≤0.01, ***p≤0.001, ****p≤0.0001. n = 3 tumors from each mouse strain; representative of 3 experiments.

References

1. Pauken, K.E. & Wherry, E.J. Overcoming T cell exhaustion in infection and cancer. *Trends Immunol* **36**, 265-276 (2015).

2. Pipkin, M.E. *et al.* Interleukin-2 and inflammation induce distinct transcriptional programs that promote the differentiation of effector cytolytic T cells. *Immunity* **32**, 79-90 (2010).

3. Cruz-Guilloty, F. *et al.* Runx3 and T-box proteins cooperate to establish the transcriptional program of effector CTLs. *J Exp Med* **206**, 51-59 (2009).

4. Shan, Q. *et al.* The transcription factor Runx3 guards cytotoxic CD8(+) effector T cells against deviation towards follicular helper T cell lineage. *Nat Immunol* **18**, 931-939 (2017).

5. Miller, B.C. *et al.* Subsets of exhausted CD8+ T cells differentially mediate tumor control and respond to checkpoint blockade. *Nature Immunology* **20**, 326-336 (2019).

6. LaFleur, M.W. *et al.* PTPN2 regulates the generation of exhausted CD8+ T cell subpopulations and restrains tumor immunity. *Nature Immunology* **20**, 1335-1347 (2019).

7. Kurtulus, S. *et al.* Checkpoint Blockade Immunotherapy Induces Dynamic Changes in PD-1−CD8+ Tumor-Infiltrating T Cells. *Immunity* **50**, 181-194 e186 (2019).

8. Im, S. *et al.* Defining CD8+ T cells that provide the proliferative burst after PD-1 therapy. *Nature* **537**, 417-421 (2016).

9. Krishna, S. *et al.* Stem-like CD8 T cells mediate response of adoptive cell immunotherapy against human cancer. *Science* **370**, 1328-1334 (2020).

10. Zhou, X. *et al.* Differentiation and Persistence of Memory CD8+ T Cells Depend on T Cell Factor 1. *Immunity* **33**, 229-240 (2010).

11. Zhou, X. & Xue, H.-H. Cutting Edge: Generation of Memory Precursors and Functional Memory CD8⁺ T Cells Depends on T Cell Factor-1 and Lymphoid Enhancer-Binding Factor-1. *The Journal of Immunology* **189**, 2722-2726 (2012).

12. Miron, M. *et al.* Human Lymph Nodes Maintain TCF-1^{hi} Memory T Cells with High Functional Potential and Clonal Diversity throughout Life. *The Journal of Immunology* **201**, 2132-2140 (2018).

13. Jeannet, G. *et al.* Essential role of the Wnt pathway effector Tcf-1 for the establishment of functional CD8 T cell memory. *Proceedings of the National Academy of Sciences* **107**, 9777-9782 (2010).

14. Utzschneider, D.T. *et al.* T Cell Factor 1-Expressing Memory-like CD8+ T Cells Sustain the Immune Response to Chronic Viral Infections. *Immunity* **45**, 415-427 (2016).

15. Ma, G., Yasunaga, J.-i., Akari, H. & Matsuoka, M. TCF1 and LEF1 act as T-cell intrinsic HTLV-1 antagonists by targeting Tax. *Proceedings of the National Academy of Sciences* **112**, 2216-2221 (2015).

16. Okamura, R.M. *et al.* Redundant regulation of T cell differentiation and TCRalpha gene expression by the transcription factors LEF-1 and TCF-1. *Immunity* **8**, 11-20 (1998).

17. Weber, B.N. *et al.* A critical role for TCF-1 in T-lineage specification and differentiation. *Nature* **476**, 63 (2011).

18. Xing, S. *et al.* Tcf1 and Lef1 transcription factors establish CD8+ T cell identity through intrinsic HDAC activity. *Nature Immunology* **17**, 695 (2016).

19. Khattar, M. *et al.* Interleukin-21 is a critical regulator of CD4 and CD8 T cell survival during priming under Interleukin-2 deprivation conditions. *PLoS One* **9**, e85882 (2014).

20. Fröhlich, A. *et al.* IL-21R on T Cells Is Critical for Sustained Functionality and Control of Chronic Viral Infection. *Science* **324**, 1576-1580 (2009).

21. Noguchi, N. *et al.* Interleukin-21 Induces Short-Lived Effector CD8(+) T Cells but Does Not Inhibit Their Exhaustion after Mycobacterium bovis BCG Infection in Mice. *Infect Immun* **86**, IAI.00147-00118 (2018).

22. Barker, B.R., Gladstone, M.N., Gillard, G.O., Panas, M.W. & Letvin, N.L. Critical role for IL-21 in both primary and memory anti-viral CD8+ T-cell responses. *Eur J Immunol* **40**, 3085-3096 (2010).

23. Novy, P., Huang, X., Leonard, W.J. & Yang, Y. Intrinsic IL-21 Signaling Is Critical for CD8 T Cell Survival and Memory Formation in Response to Vaccinia Viral Infection. *The Journal of Immunology* **186**, 2729-2738 (2011).

24. Zheng, X. *et al.* IL-21 receptor signaling is essential for control of hepatocellular carcinoma growth and immunological memory for tumor challenge. *OncoImmunology* **7**, e1500673 (2018).

25. Mittal, D. *et al.* Improved Treatment of Breast Cancer with Anti-HER2 Therapy Requires Interleukin-21 Signaling in CD8⁺ T Cells. *Cancer Research* **76**, 264-274 (2016).

26. Wang, L.N., Cui, Y.X., Ruge, F. & Jiang, W.G. Interleukin 21 and Its Receptor Play a Role in Proliferation, Migration and Invasion of Breast Cancer Cells. *Cancer Genomics Proteomics* **12**, 211-221 (2015).

27. Linnebacher, A. *et al.* Interleukin 21 Receptor/Ligand Interaction Is Linked to Disease Progression in Pancreatic Cancer. *Cells* **8** (2019).

28. Davis, M.R., Zhu, Z., Hansen, D.M., Bai, Q. & Fang, Y. The role of IL-21 in immunity and cancer. *Cancer letters* **358**, 107-114 (2015).

29. Lynn, R.C. *et al.* c-Jun overexpression in CAR T cells induces exhaustion resistance. *Nature* **576**, 293-300 (2019).

30. Chen, J. *et al.* NR4A transcription factors limit CAR T cell function in solid tumours. *Nature* **567**, 530-534 (2019).

31. Yao, C. *et al.* BACH2 enforces the transcriptional and epigenetic programs of stem-like CD8+ T cells. *Nature Immunology* **22**, 370-380 (2021).

32. Ha, N. *et al.* HP-1gamma Controls High-Affinity Antibody Response to T-Dependent Antigens. *Frontiers in immunology* **5**, 271 (2014).

33. Sun, M. *et al.* Cbx3/HP1gamma deficiency confers enhanced tumor-killing capacity on CD8+ T cells. *Sci Rep* **7**, 42888 (2017).

34. Maekawa, Y. *et al.* Notch2 integrates signaling by the transcription factors RBP-J and CREB1 to promote T cell cytotoxicity. *Nature Immunology* **9**, 1140-1147 (2008).

35. Berrien-Elliott, M.M. *et al.* Checkpoint Blockade Immunotherapy Relies on T-bet but Not Eomes to Induce Effector Function in Tumor-Infiltrating CD8⁺ T Cells. *Cancer Immunology Research* **3**, 116-124 (2015).

36. Knudson, K.M. *et al.* NFκB–Pim-1–Eomesodermin axis is critical for maintaining CD8 T-cell memory quality. *Proceedings of the National Academy of Sciences* **114**, E1659-E1667 (2017).

37. Le, T.P. & Thai, T.H. The State of Cellular Adoptive Immunotherapy for Neuroblastoma and Other Pediatric Solid Tumors. *Frontiers in immunology* **8**, 1640 (2017).

38. Matulonis, U.A. *et al.* Antitumor activity and safety of pembrolizumab in patients with advanced recurrent ovarian cancer: results from the phase II KEYNOTE-100 study. *Ann Oncol* **30**, 1080-1087 (2019).

39. Martin, S.D. *et al.* Low Mutation Burden in Ovarian Cancer May Limit the Utility of Neoantigen-Targeted Vaccines. *PLoS One* **11**, e0155189 (2016).

40. Chen, X. *et al.* CCL2/CCR2 Regulates the Tumor Microenvironment in HER-2/neu-Driven Mammary Carcinomas in Mice. *PLOS ONE* **11**, e0165595 (2016).

41. Chheda, Z.S., Sharma, R.K., Jala, V.R., Luster, A.D. & Haribabu, B. Chemoattractant receptors BLT1 and CXCR3 regulate antitumor immunity by facilitating CD8(+) T cell migration into tumors. *Journal of immunology (Baltimore, Md. : 1950)* **197**, 2016-2026 (2016).

42. Liu, J. *et al.* Local production of the chemokines CCL5 and CXCL10 attracts CD8(+) T lymphocytes into esophageal squamous cell carcinoma. *Oncotarget* **6**, 24978-24989 (2015).

43. Ramakrishnan, R. *et al.* CXCR4 Signaling Has a CXCL12-Independent Essential Role in Murine MLL-AF9-Driven Acute Myeloid Leukemia. *Cell Rep* **31**, 107684 (2020).

44. Facciabene, A. *et al.* Tumour hypoxia promotes tolerance and angiogenesis via CCL28 and T(reg) cells. *Nature* **475**, 226-230 (2011).

45. Acharya, N. *et al.* Endogenous Glucocorticoid Signaling Regulates CD8+ T Cell Differentiation and Development of Dysfunction in the Tumor Microenvironment. *Immunity* **53**, 658-671.e656 (2020).

46. Sade-Feldman, M. *et al.* Defining T Cell States Associated with Response to Checkpoint Immunotherapy in Melanoma. *Cell* **175**, 998-1013.e1020 (2018).

47. Carr, T. *et al.* The transcription factor lymphoid enhancer factor 1 controls invariant natural killer T cell expansion and Th2-type effector differentiation. *Journal of Experimental Medicine* **212**, 793-807 (2015).

48. Reya, T. *et al.* Wnt Signaling Regulates B Lymphocyte Proliferation through a LEF-1 Dependent Mechanism. *Immunity* **13**, 15-24 (2000).

Methods

Mice

Cbx3/HP1γ floxed mice were generated and provided by Dr. Prim B. Singh[1]. These mice were backcrossed to C57BL/6 for twelve generations; they bred and developed normally before and after Cre-mediated deletion. The *Cbx3*/HP1γ transgenic line was generated by inserting a 1 kb fragment of mouse *Cbx3*/HP1γ cDNA, derived from activated $CD8^+$ T cells, into EcoR1/Sma1 cloning sites of the VA-hCD2 vector provided by Dr. Dimitris Kioussis[2]. The purified *Cbx3*/HP1γ-VA-hCD2 DNA construct was injected into C57BL/6 pronuclei by Dr. Lina Du at the fee-based Dana-Farber/Harvard Cancer Center (DF/HCC) Transgenic Mouse Core. Two founder transgenic lines were produced. The *Lef1* floxed mice were generated as described and provided by Dr. Hai-Hui Xue[3]. The following mouse lines were purchased from The Jackson Laboratory: *Tcf7* floxed (B6(Cg)-*Tcf7*^{tm1Hhx}/J)[4], *Il21r* knock out (B6.129-*Il21r*^{tm1Kopf}/J)[5], CD8α-Cre transgenic (C57BL/6-Tg(Cd8a-cre)1Itan/J)[6], ROSA26 (B6;129-*Gt(ROSA)26Sor*^{tm2Sho}/J)[7], *Prf1* knock out (C57BL/6-*Prf1*^{tm1Sdz}/J)[8], and *Ifng* knock out (B6.129S7-*Ifng*^{tm1Ts}/J)[9]. The B6.SJL line (B6.SJL-*Ptprc*^{a}/BoyAiTac) was purchased from Taconic. All mice were maintained in specific pathogen-free (SPF) conditions. All mouse protocols were approved by the BIDMC Institutional Animal Care and Use Committee. All experiments were performed in accordance with relevant guidelines and regulations.

Tumor cell lines.

The mouse syngeneic ID8 ovarian tumor line was obtained from Dr. Katherine F. Roby under an MTA executed by the University of Kansas Medical Center[10]. Dr. Eva M. Schmelz provided the mouse syngeneic MOSE-L_{TICv} ovarian tumor line[11, 12]. The NB9464 neuroblastoma cell line was a kind gift from Dr. Crystal L. MacKall (Stanford University)[13]. The B16-F10 melanoma cell line was purchased from ATCC and tested negative for mycoplasma.

Antibodies

All flow cytometry fluorochrome-conjugated antibodies were purchased from BioLegend, eBio-sciences or BD Biosciences. The following Western blot and ChIP-tested antibodies were purchased from Cell Signaling: tri-methyl-histone H3 (Lys9) (D4W1U) rabbit mAb #13969, phospho-Rpb1 CTD (Ser2) (E1Z3G) rabbit mAb #13499, phospho-Rpb1 CTD (Ser5) (D9N5I) rabbit mAb #13523, LEF-1 (C12A5) rabbit mAb #2230, cleaved caspase-3 (Asp175) antibody #9661 and phospho-HP1γ (Ser83) Ab #2600. The Western blot and ChIP-tested mouse anti-HP1γ

mAb (clone 42s2) was purchased from Millipore Sigma. The rabbit polyclonal to TBR2/Eomes (ab23345) was purchased from Abcam. The rat mAb to mouse granzyme B (16G6) was from Invitrogen/ThermoFisher Scientific.

Tumor induction

Ovarian cancer

Mice were injected intraperitoneally (IP) with ID8 (5 x 10^6/mouse in 200 µl PBS) or MOSE-L_{TICv} (1 x 10^4/mouse in 200 µl PBS). On day 120 (ID8) or 36 (MOSE-L_{TICv}), when abdominal distension was visible, mice were euthanized, ascites were collected, and volume measured using syringes fitted with 18-gauge needles.

Melanoma

Mice were implanted subcutaneously with B16 tumor cells (1 x 10^5/mouse in 100µL PBS). Using a digital caliber, B16 tumor size was measured and calculated on day 14 and at 2-day or 3-day intervals until day 20 depending on the size of the tumor, at which time mice were euthanized for analysis.

Neuroblastoma

Mice were implanted subcutaneously with NB-9464 tumor cells (1 x 10^6/mouse in 100µL PBS). Using a digital caliber, NB-9464 tumor volume was measured and calculated (W x L x 0.4) starting on day 22 and at 2-day intervals until day 30 depending on the size of the tumor, at which time mice were euthanized for analysis.

Fluorescence-activated cell sorting or flow cytometry (FACS)

FACS was performed on the BD 5-laser LSR II or the Beckman Coulter CytoFLEX LX. Analysis was performed with FlowJo software (Tree Star, Inc.). Tumors and ascites were harvested, minced (NBL and melanoma), and cell-suspensions were filtered through 70µm cell-strainers (Fisherbrand). Cells were stained for appropriate surface markers as indicated in figures.

***In vitro* differentiation of $CD8^+$ T cells**

$CD8^+CD44^-$ T cells were purified from spleen and peripheral lymph nodes using the MojoSort™ Mouse CD8 Naïve T-Cell Isolation Kit (BioLegend, #480044) followed by CD25-depletion using the mouse CD25 MicroBead Kit (Miltenyl Biotec, #130-091-072), all according manufacturers' protocols. Naïve $CD8^+$ T cells (1 × 10^6/mL) were activated with plate-bound anti-CD3 (clone 145-2C11, 0.25 µg/ml, BioLegend) and anti-CD28 (clone 37.51, 0.5 µg/ml,

BioLegend) in T-cell medium (high glucose DMEM, 10% FBS, penicillin/streptomycin, non-essential amino acids, HEPES, L-glutamate and sodium pyruvate) at 37°C in 10% CO_2 for 2 days. Cells were then removed from CD3/CD28 activation and re-cultured (5×10^5/ml) in differentiation medium (T-cell medium supplemented with 10 IU/ml rhIL-2 from NCI) at 37°C in 10% CO_2. Cells were then sub-cultured every day in differentiation medium at 5×10^5/ml each sub-culture. On day 5, cells were harvested and used for Western blots, ChIP-qPCR, qPCR or adoptive T-cell therapy.

Adoptive T-cell transfer

In vitro-generated donor $CD8^+$ effector T cells ($CD45.2^+$) were prepared as above. On day 0, B6.SJL ($CD45.1^+$) mice were implanted subcutaneously with NB-9464 (1 x 10^6/mouse in 100µL PBS) or B16 (1 x 10^5/mouse in 100µL PBS) tumor cells. On day 10 (B16) or 14 (NB-9464) after tumor induction, mice were treated with donor $CD8^+$ effector T cells (3 x 10^6/mouse in 100µL PBS) via tail vein intravenous injection. B16 tumor size and NB-9464 tumor volume were measured and calculated on indicated dates.

Co-culturing effector cells with B16 tumor cells

Target B16 tumor cells were plated in 12-well plates at a density of 5 x 10^5 cells per well in 750µl of medium (high glucose DMEM, 10% FBS, penicillin/streptomycin, non-essential amino acids, HEPES, L-glutamate and sodium pyruvate). $CD8^+$ or $CD4^+$ effector T cells were added. For ratio of 1:1 (effector:target), 5 x 10^5 $CD8^+$ or $CD4^+$ T cells: 5 x 10^5 B16 cells were co-cultured in the same well; ratio 5:1, 2.5 x 10^6 $CD8^+$ or $CD4^+$ T cells: 5 x 10^5 B16 cells. Plates were incubated at 37°C in 5% CO_2 for 24 hours. Wells were washed to remove non-adherent T cells. Adherent B16 cells were collected and washed with 1 ml cold PBS. Pellets were resuspended in Radio-Immunoprecipitation Assay (RIPA) lysis buffer containing a protease inhibitor cocktail (Roche) and used immediately or stored at –80°C for further analysis.

Western Blots

Cells (1 x 10^6) were lysed with RIPA buffer (Boston BioProducts) containing a protease inhibitor cocktail on ice for 30 minutes. Lysates were centrifuged at 13,000 rpm for 10 minutes at 4°C. Protein extracts were denatured at 95°C for 10 minutes, separated by SDS-PAGE, and transferred to PVDF membranes (EMD Millipore). Membranes were probes with primary antibodies. Proteins of interest were detected with HRP-conjugated secondary antibodies and the Pierce™ ECL

Western Blotting Substrate (ThermoFisher Scientific). Membranes were exposed with HyBlot CL Autoradiography films (Denville Scientific, Inc.), and developed with the Kodax X-OMAT 2000 Processor.

Chromatin immunoprecipitation followed by qPCR (ChIP-qPCR) and ChIP followed by deep sequencing (ChIP-Seq)

ChIP-qPCR

ChIP was performed using the SimpleChIP Kit #9003 according to manufacturer's protocol (Cell Signaling). Briefly, 2 x 10^7 $CD8^+$ T cells were used for each ChIP. Cells were fixed in 1% formaldehyde to cross-link proteins to DNA, then lysed with 500µL of lysis buffer containing 1X ChIP buffer and protease inhibitor cocktail. Chromatin was sheared using a Sonic Dismembrator (Fisher Scientific Model 120) at 120W-20kHz power, at 15 seconds per cycle, 45 seconds break in between, for 3 cycles total. Chromatin was subjected to immunoprecipitation using specific antibodies at 4°C overnight with rotation. Following incubation, ChIP grade protein G magnetic beads were added to each ChIP and incubated for 2 hours at 4°C with rotation. Samples were placed in a magnetic separation rack for 2 minutes each time and washed 3X with high and low salt buffers. Chromatin was eluted from antibody/protein G magnetic beads using 1X ChIP elution buffer at 65°C for 30 minutes. Eluted chromatin was collected and subjected to cross-link reversal using 5M NaCl and 20 mg/ml Proteinase K, incubated for 2 hours at 65°C. After reversal of protein-DNA cross-link, the DNA was purified using DNA purification spin columns and eluted with DNA elution buffer provided in the kit. Purified ChIP DNA was immediately used for qPCR using primers shown in Table S3. BioRad hard-shell PCR Plates (BioRad) were used. In each well 2µL of purified ChIP DNA was added in triplicates along with 18µl primer mixture, which consisted of 1µL forward primer (5µM), 1µL reverse primer (5µM), 6µL nuclease-free water, and 10µL of 2X QuaniNova SYBR Green PCR Master Mix (Qiagen) or SimpleChIP Universal qPCR Master Mix (Cell Signaling). The plate was centrifuged at 300 RCF for 1 minute and read in the BioRad CFX384 Real-Time System (BioRad). The following qPCR settings were used: initial denaturation 95°C for 3:00 minutes, denatured at 95°C for 0:15 minutes, annealing and extension at 60°C for 1:00 minute, GOTO step denature and extension for a total of 40 cycles. Quantitative PCR result was analyzed, and the IP efficiency was calculated per formula provided in Simple ChIP Kit #9003 (Cell Signaling). Primers are listed in Extended Data Table 3.

ChIP-Seq

Detailed experiments and analyses have been described previously[14].

Reverse transcription-quantitative polymerase chain reaction (RT-qPCR).

The BioRad hard-shell PCR Plates (BioRad) were used. In each well 2.5µL of sample was added in triplicates along with 7.5µL of the primer mixture (Table S2), which consisted of 0.5µL forward primer (10µM), 0.5µL reverse primer (10µM), 1.7µL PCR grade water, and 5µL of Roches LightCycler 480 SYBR Green I Master (Roche). The plate was centrifuged at 300 RCF for 1 minute and read in the BioRad CFX384 Real-Time System (BioRad). The qPCR settings: 95°C for 10:00 minutes, 95°C for 0:10 minutes, 62°C for 0:20 minutes, 72°C for 0:20 minutes (Read Plate), GOTO step 2 for 39 times, 92°C for 0:05 minutes, melt curve 65°C to 97°C, at increment of 0.5°C for 1:00 minute (Read Plate), 40°C for 0:10 minutes. Primers are listed in Extended Data Table 2.

Immunohistochemistry (IHC)

Tumor section processing and TUNEL staining were performed by HistoWiz (Brooklyn, NY). Briefly, all IHC staining is automated using BOND Rx. Slides were treated with Dewax, a solvent-based solution (Leica Biosystems). Tissue sections were fixed by adding 10% neutral buffered formalin for 15 minutes. Slides were treated with Proteinase K at 1:500 dilution. Tissue sections were re-fixed using 10% neutral buffered formalin. Tissue sections were then treated with the equilibration buffer and incubated for 12 minutes at room temperature (RT). Subsequently the TdT reaction mix was added and incubated for 60 minutes at 37°C. The TUNEL reaction was stopped by adding 2X SSC. Tissue slides were treated with Peroxide Block (3-4% Hydrogen Peroxide) followed by wash buffer. Streptavidin HRP was added and incubated for 30 minutes at RT. DAB was added onto the slides and incubated for 10 minutes. Counter-staining was done by adding hematoxylin. Slides were covered using the Sakura Tissue Tek strainer and cover slips then scanned at 40x using the Leica AT2 scanner.

References

1. Oyama, K. *et al.* Deletion of HP1gamma in cardiac myocytes affects H4K20me3 levels but does not impact cardiac growth. *Epigenetics & chromatin* **11**, 18 (2018).

2. Zhumabekov, T., Corbella, P., Tolaini, M. & Kioussis, D. Improved version of a human CD2 minigene based vector for T cell-specific expression in transgenic mice. *J Immunol Methods* **185**, 133-140 (1995).

3. Zhou, X. & Xue, H.-H. Cutting Edge: Generation of Memory Precursors and Functional Memory CD8⁺ T Cells Depends on T Cell Factor-1 and Lymphoid Enhancer-Binding Factor-1. *The Journal of Immunology* **189**, 2722-2726 (2012).

4. Yang, Q. *et al.* TCF-1 upregulation identifies early innate lymphoid progenitors in the bone marrow. *Nature Immunology* **16**, 1044-1050 (2015).

5. Frohlich, A. *et al.* IL-21 receptor signaling is integral to the development of Th2 effector responses in vivo. *Blood* **109**, 2023-2031 (2007).

6. Maekawa, Y. *et al.* Notch2 integrates signaling by the transcription factors RBP-J and CREB1 to promote T cell cytotoxicity. *Nature Immunology* **9**, 1140-1147 (2008).

7. Mao, X., Fujiwara, Y., Chapdelaine, A., Yang, H. & Orkin, S.H. Activation of EGFP expression by Cre-mediated excision in a new ROSA26 reporter mouse strain. *Blood* **97**, 324-326 (2001).

8. Kagi, D. *et al.* Cytotoxicity mediated by T cells and natural killer cells is greatly impaired in perforin-deficient mice. *Nature* **369**, 31-37 (1994).

9. Dalton, D.K. *et al.* Multiple defects of immune cell function in mice with disrupted interferon-gamma genes. *Science* **259**, 1739-1742 (1993).

10. Roby, K.F. *et al.* Development of a syngeneic mouse model for events related to ovarian cancer. *Carcinogenesis* **21**, 585-591 (2000).

11. Cohen, C.A., Shea, A.A., Heffron, C.L., Schmelz, E.M. & Roberts, P.C. The Parity-Associated Microenvironmental Niche in the Omental Fat Band Is Refractory to Ovarian Cancer Metastasis. *Cancer Prevention Research* **6**, 1182-1193 (2013).

12. Roberts, P.C. *et al.* Sequential Molecular and Cellular Events during Neoplastic Progression: A Mouse Syngeneic Ovarian Cancer Model. *Neoplasia* **7**, 944-956 (2005).

13. Kroesen, M. *et al.* A transplantable TH-MYCN transgenic tumor model in C57Bl/6 mice for preclinical immunological studies in neuroblastoma. *International journal of cancer. Journal international du cancer* **134**, 1335-1345 (2014).

14. Sun, M. *et al.* Cbx3/HP1gamma deficiency confers enhanced tumor-killing capacity on CD8+ T cells. *Sci Rep* **7**, 42888 (2017).

Figures

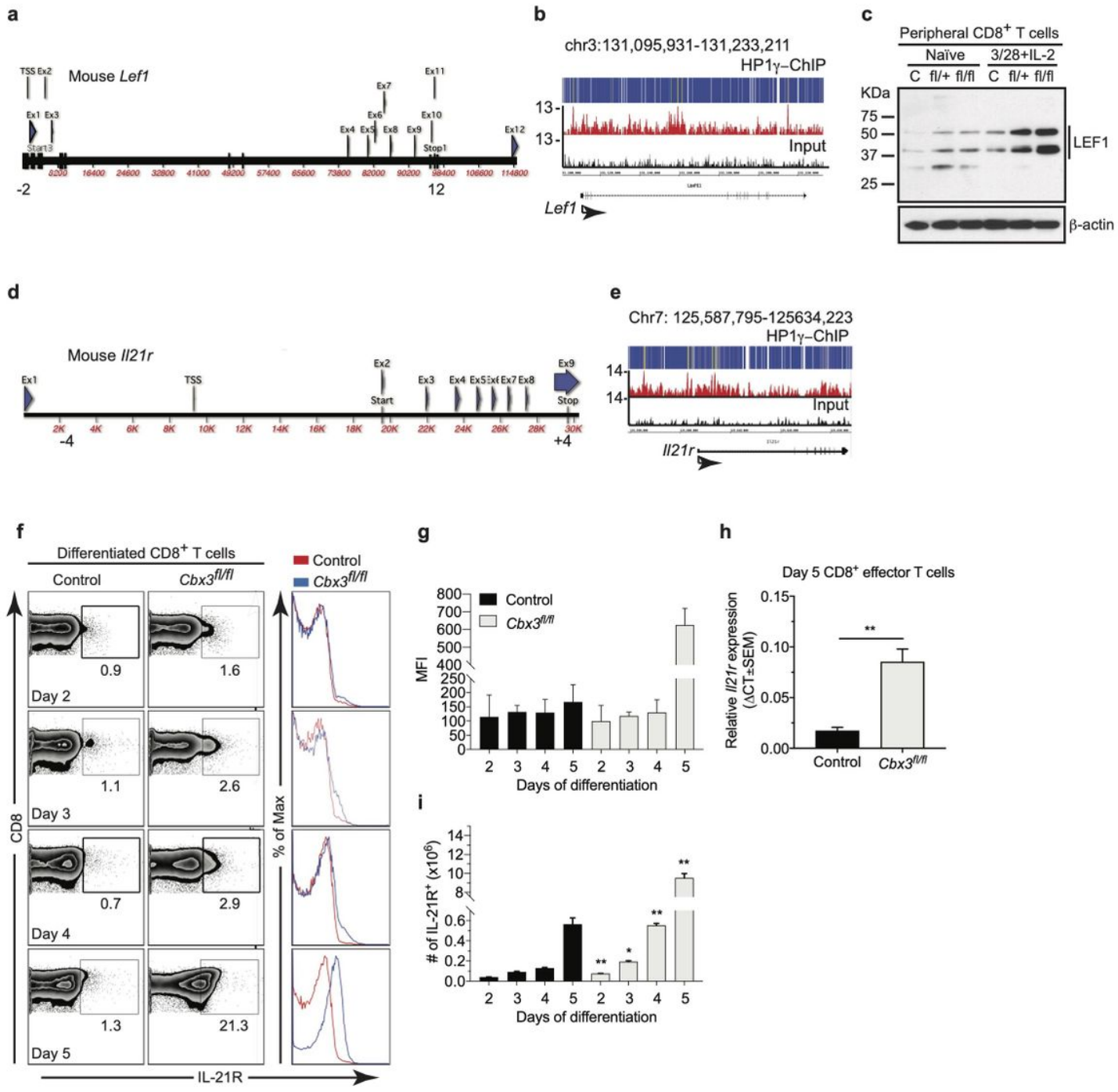

Figure 1

Cbx3/HP1g deficiency modulates LEF-1 and IL-21R expression in CD8+ effector T cells. a, Schematic of mouse Lef1 locus. -2 and 12 indicated positions of first and last primer pairs, respectively. b, Read-density tracks of Cbx3/HP1g peaks across Lef1 identified by ChIP-Seq using chromatin from wt day 5 differentiated CD8+ T cells (as in c, pooled from 3 mice); y axis: number of reads per million mapped per

25-bp window. c, LEF-1 expression was assessed by Western immunoblot using total lysates from differentiated control and Cbx3/HP1g-deficient CD8+ T cells; 3/28+IL2: CD8+ T cells differentiated for 5 days with plate-bound anti-CD3 and anti-CD28 plus IL-2; C: control (CD8a-Cre or wt); fl/+: Cbx3fl/+; fl/fl: Cbx3fl/fl: CD8+ T-cell-restricted deletion of Cbx3/HP1g using the CD8a-Cre mouse. d, Schematic of mouse Il21r locus. -4 and 4: positions of first and last pair of primers, respectively. e, Read-density tracks of Cbx3/HP1g peaks across Il21r identified by ChIP-Seq as in (b). f, IL-21R expression on differentiated CD8+ T cells was determined by flow cytometry; left panels depicted percent CD8+IL-21R+ cells from each culture; right panels indicated IL-21R levels on the same cells; numbers: percent cells; representative of 3 experiments; n = 3 for each genotype. g, Graphs represented IL-21R mean fluorescence intensity (MFI) from (f). h, Relative expression of Il21r, normalized to Gapdh, in day 5 differentiated CD8+ T cells was evaluated by RT-qPCR using RNA from cells obtained in (f); Graphpad unpaired student t-test: **p£0.01; representative of 3 experiments. i, Number of CD8+IL-21R+ T cells in cultures were calculated from (f); Graphpad unpaired student t-test: *p£0.05, **p£0.01.

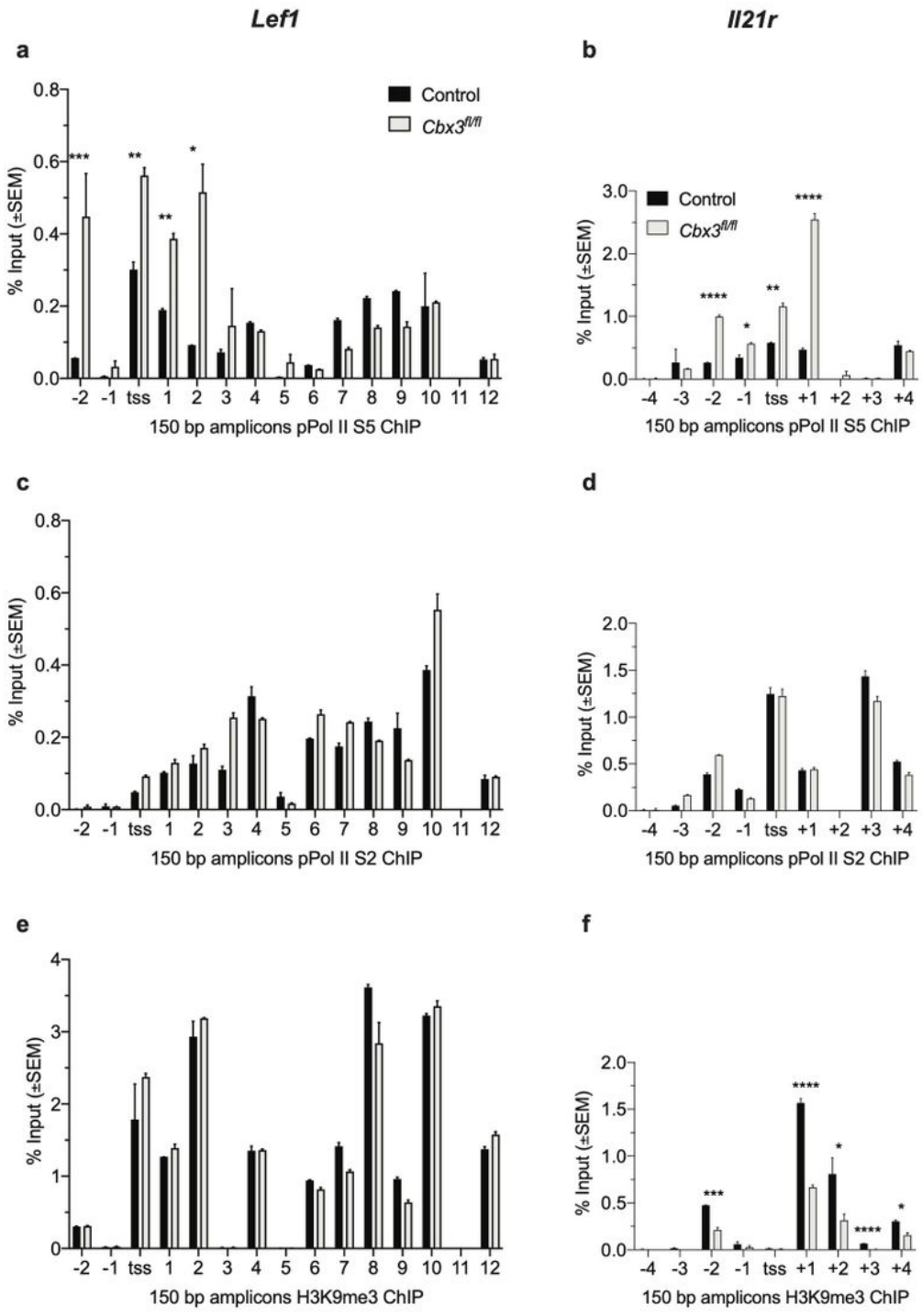

Figure 2

Cbx3/HP1g regulates Lef1 and Il21r transcription initiation and chromatin remodeling. a,b, Levels of Pol II S5 bound to Lef1 (a) and Il21r (b) were quantified by ChIPqPCR using chromatin from day 5 differentiated CD8+ T cells. TSS: transcription start site, numbers on X axis: positions of primers along the two loci; 150 bp products amplified by Lef1 or Il21r primers. c,d, Levels of Pol II S2 bound to Lef1 (c) and Il21r (d) were quantified as in (a,b). e,f, H3K9me3 deposition on Lef1 (e) and Il21r (f) was quantified

as in (a,b). Statistics: Graphpad unpaired student t-test: *p£0.05, **p£0.01, ***p£0.001, ****p£0.0001; representative of 4 independent ChIPs using pooled chromatin from 3 mice.

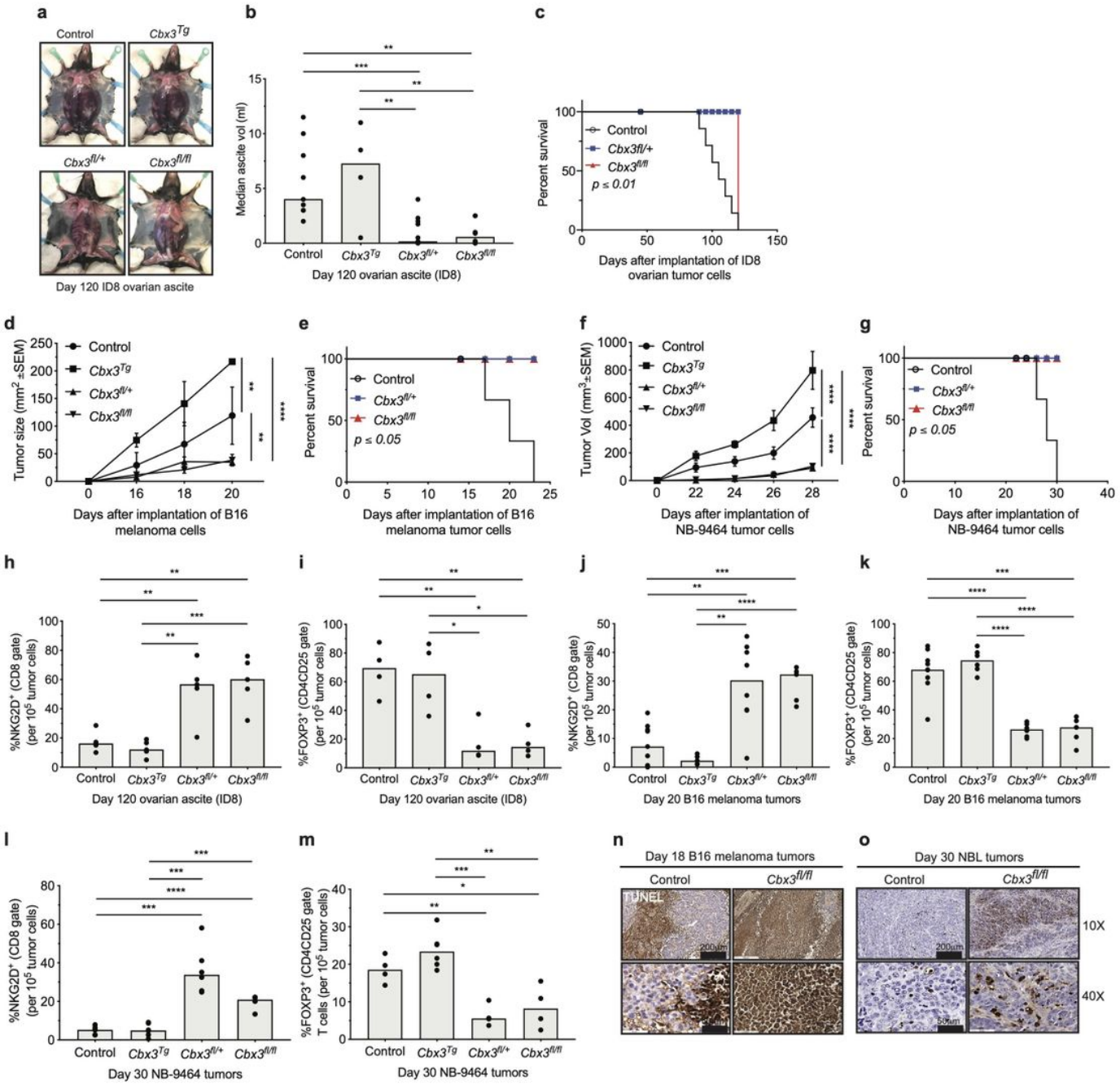

Figure 3

Cbx3/HP1g-deficient CD8+ effector T cells can persist and cause tumor rejection. a, Ascites from control (CD8a-Cre or wt), Cbx3Tg, Cbx3fl/+ and Cbx3fl/fl mice (X axis) were visualized on day 120 after intraperitoneal injection of mouse ID8 ovarian tumor cells; Cbx3Tg: Cbx3/HP1g T-cell-restricted expression driven by the human Cd2 promoter; Cbx3fl/+ and Cbx3fl/fl: CD8+ T-cell-restricted deletion of Cbx3/HP1g using the CD8a-Cre mouse. b, Ovarian ascites (vol: volume) of mice in (a) were measured and

graphed; bars: group median; Graphpad unpaired student t-test: **p£0.01, ***p£0.001; each symbol = one mouse; n = 5-8. c, Survival curves of ovarian tumor-bearing mice were determined; Graphpad log-rank (Mantel-Cox) test; n = 5-8. d, B16 tumor cells were injected subcutaneously (sc) and growth was assessed starting on day 14 after tumor-cell injection then every 2 days through day 20; Graphpad two-way ANOVA: **p£0.01, ****p£0.0001; n = 5. e, Survival curves of B16 melanoma tumor-bearing mice.; Graphpad log-rank (Mantel-Cox) test; n = 5. f, NB-9464 tumor cells were injected sc, NBL tumor growth was determined every 2 days starting on day 22 through day 28; Graphpad two-way ANOVA: ****p£0.0001; n = 5. g, Survival curves of NBL tumor-bearing mice; Graphpad logrank (Mantel-Cox) test, n = 5. h,j,l, Frequencies of CD8+NKG2D+ T cells in ovarian ascites, B16 and NBL tumors from control (CD8a-Cre or wt), Cbx3Tg, Cbx3fl/+ and Cbx3fl/fl mice; data were extracted from flow analysis (Extended Data Fig. 2c,e,g); bars: group median; Graphpad unpaired student t-test: **p£0.01, ***p£0.001, ****p£0.0001; each symbol = one mouse; n = 5-8. j,k,m, Frequencies of CD4+FOXP3+ Tregs in ovarian ascites, B16 and NBL tumors (Extended Data Fig. 2d,f,h); bars: group median; Graphpad unpaired student t-test: *p£0.05, **p£0.01, ***p£0.001, ****p£0.0001; each symbol = one mouse; n = 5-8 for each genotype. n,o, Apoptotic cells (brown) in B16 melanoma and NBL tumor sections were identified by TUNEL staining; representative of 4 tumors from each mouse strain.

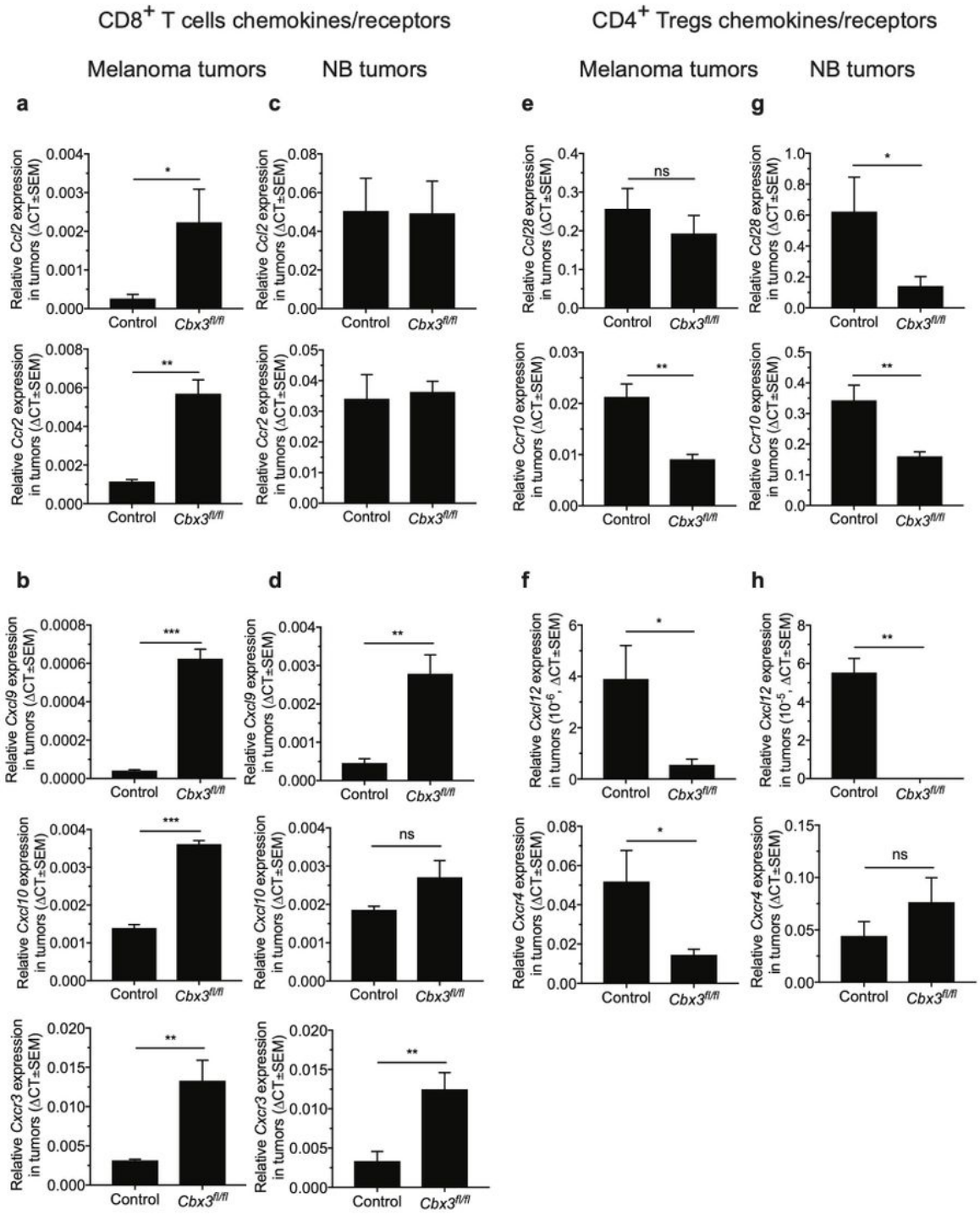

Figure 4

Cbx3/HP1g-deficient CD8+ T cells remodel the tumor chemokine/receptor landscape. a,b, Relative expression of chemokines and receptors mediating CD8+ T cells trafficking into B16 tumors were measured by RT-qPCR using RNA of day 5 differentiated CD8+ T cells from control and Cbx3/HP1g-deficient CD8+ T cells as in figure 1c, results were normalized to Gapdh. c,d, Relative expression of chemokines and receptors mediating CD8+ T cells trafficking into NBL tumors. e,f, Relative expression of

chemokines and receptors inducing CD4+ Tregs homing into B16 tumors normalized to Gapdh. g,h, Relative expression of chemokines and receptors inducing CD4+ Tregs homing into NBL tumors. X axis: mouse strains; Graphpad unpaired student t-test: *p£0.05, **p£0.01, ***p£0.001; ns: not significant; n = 4 tumors from each mouse strain.

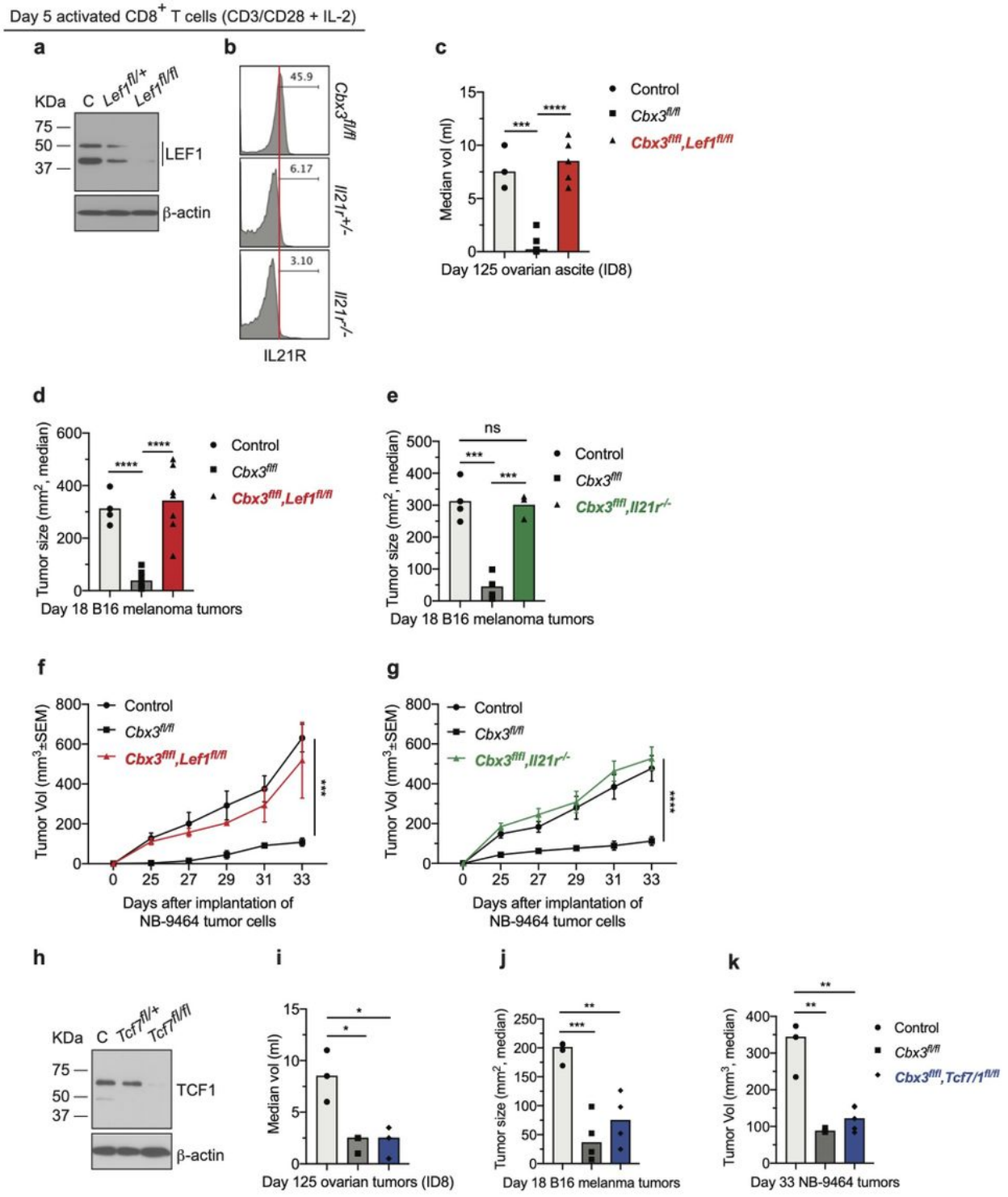

Figure 5

LEF-1 and IL-21R are indispensable for halting tumor growth. a, Western blot of LEF-1 expression was done using total lysates of day 5 differentiated CD8+ T cells; C: Cbx3/HP1gdeficient; Lef1fl/+ and Lef1fl/fl: Cbx3-Lef1-deficient. b, IL-21R expression was evaluated by flow; Cbx3fl/fl: Cbx3/HP1g-deficient; Il21r+/- and Il21r-/-: Cbx3-Il21r-deficient. c, Ovarian ascites were measured on day 125 after tumor injection; bars: group median; Graphpad unpaired student t-test: ***p£0.001, ****p£0.0001; each symbol = one mouse; n = 3-5. Cbx3fl/flLef1fl/fl: Cbx3-Lef1- deficient. d, B16 melanoma tumor burden was determined on day 18 after tumor injection; bars: group median; Graphpad unpaired student t-test: ****p£0.0001; each symbol = mouse; for each genotype n = 4-7. e, On day 10 after injection of tumor cells, tumor bearing B6SJ/L mice were treated with in vitro-differentiated CD8+ T cells from control, Cbx3fl/f or Cbx3fl/f,Il21r-/- (Cbx3- Il21r-deficient); ***p£0.001, n = 3-4 recipients. f, NBL tumor burden was determined starting on day 25 after injection of tumor cells then every 2 days until day 33; Graphpad two-way ANOVA: ***p£0.001; n = 2-5. g, On day 14 after NBL injection, tumor bearing B6SJ/L mice were treated with in vitro-differentiated CD8+ T cells from control, Cbx3fl/f or Cbx3fl/f,Il21r-/- (Cbx3-Il21rdeficient); ****p£0.0001, n = 3-4 recipients. h, Western blot of TCF-1 expression was done using total lysates of day 5 differentiated CD8+ T cells; C: Cbx3/HP1g-deficient; Tcf7fl/+ and Tcf7fl/fl: Cbx3-Tcf7-deficient. i-k, Ovarian ascites (i), B16 tumor size (j) and NBL tumor volume (k) were measured in control, Cbx3/HP1g-deficient and Cbx3-Tcf7-deficient mice; Graphpad unpaired student t-test: *p£0.05, **p£0.01, ***p£0.001; n = 3-4 per genotype.

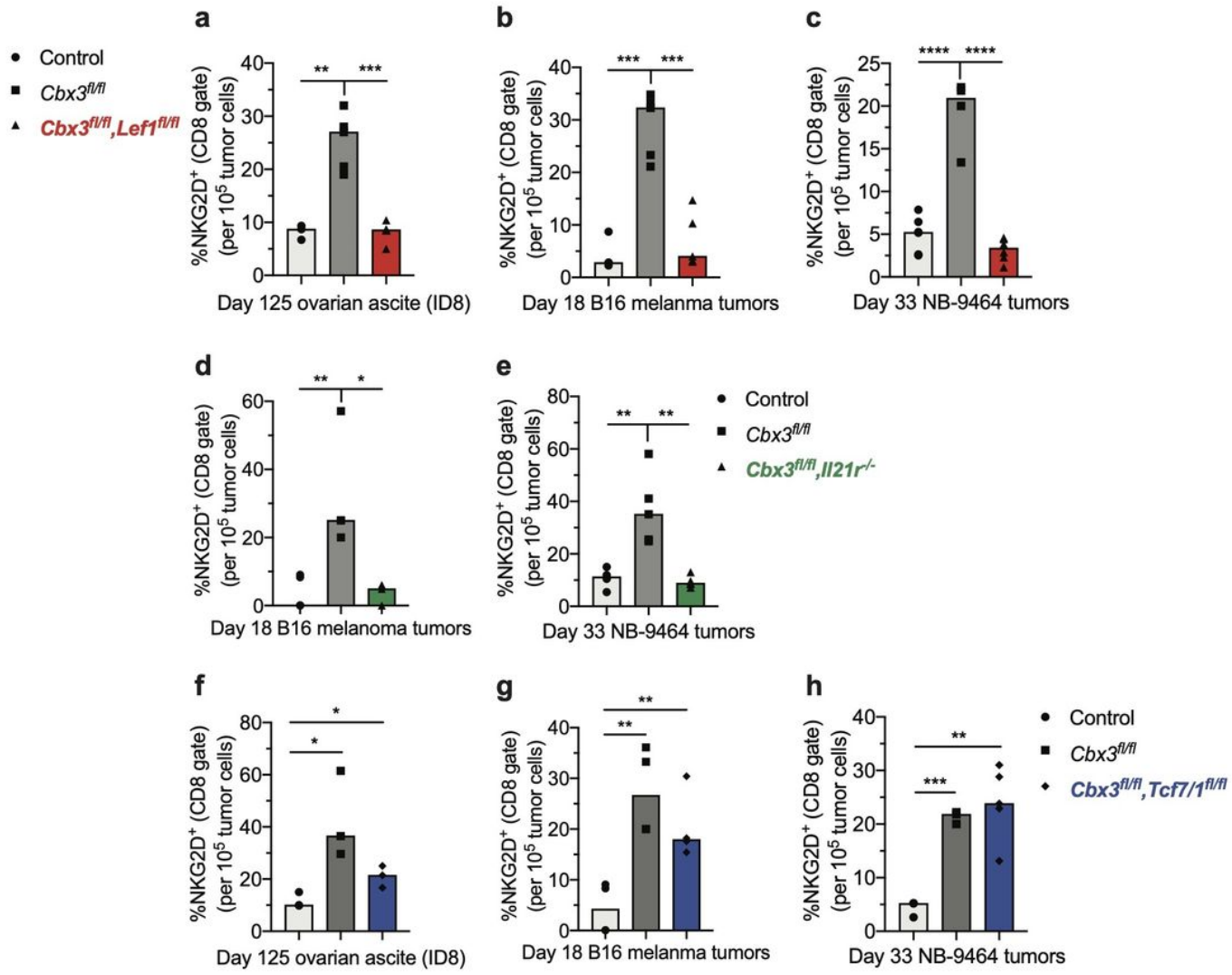

Figure 6

LEF-1 and IL-21R are required for Cbx3/HP1g-deficient CD8+ effector T cells to persist in tumors. a,b,c, Frequencies of CD8+NKG2D+ T cells in ovarian ascites (a), B16 (b) and NBL (c) tumors were determined using data extracted from flow analysis. d,e, Frequencies of CD8+NKG2D+ T cells (gated on CD45.2+ populations) in B16 melanoma (d) and NBL (e) tumors from B6.SJL mice treated with in vitro-differentiated control, Cbx3/HP1g- or Cbx3-Lef1-deficient CD8+ effector T cells on day 10 and day 14 after injection of B16 and NBL tumor cells, respectively. f-h, ovarian ascites (f), B16 tumor size (g) and NBL tumor volume (h) of control, Cbx3/HP1g- or Cbx3-Tcf7-deficient mice. Statistics: bars: group median; Graphpad unpaired student t-test: *p£0.05, **p£0.01, ***p£0.001, ****p£0.0001; each symbol = one mouse; n = 3- 5.

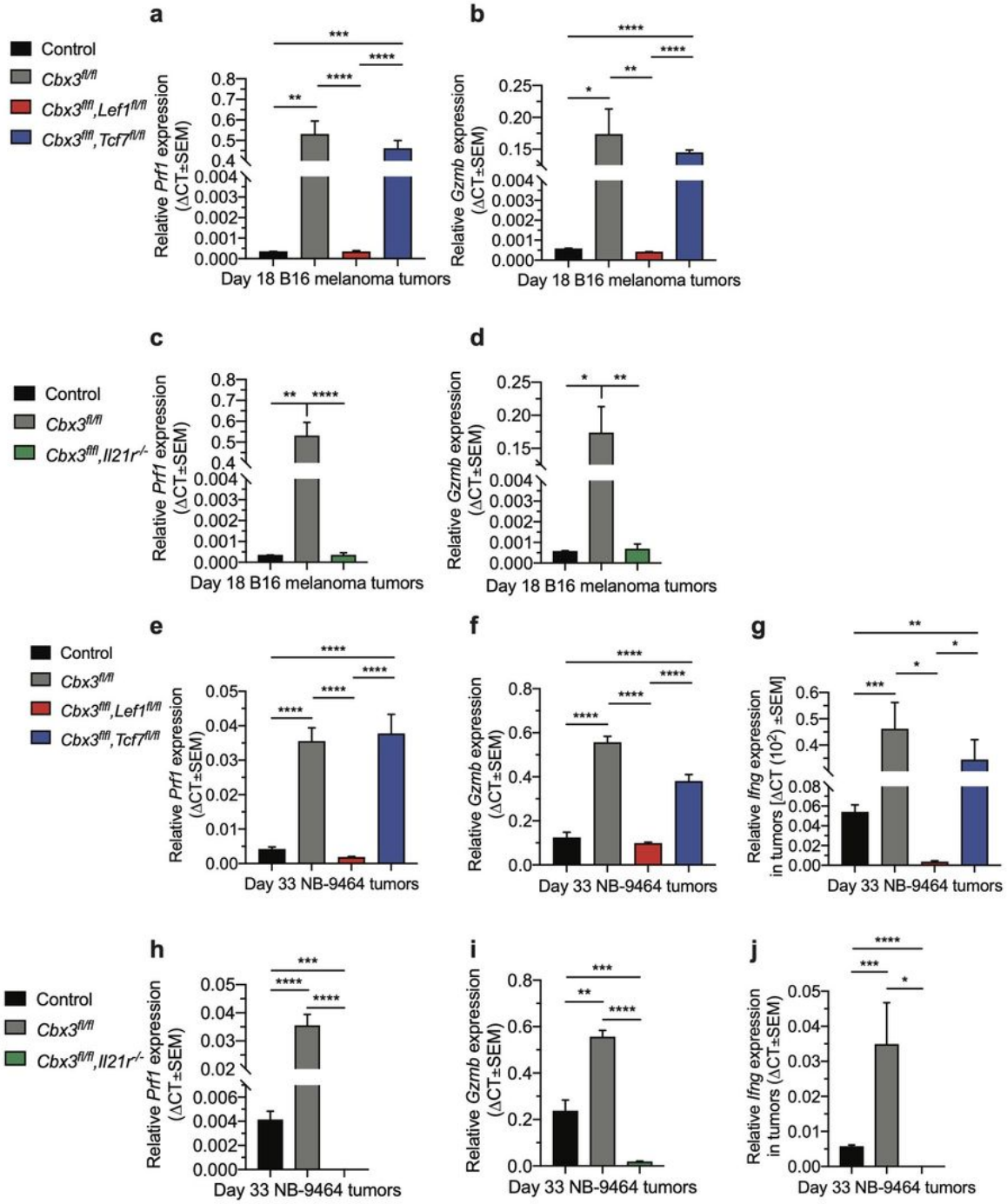

Figure 7

LEF-1 and IL-21R are required to maintain effector activity in tumors. a,b, Prf1 and Gzmb relative expression in day 18 B16 melanoma tumors was quantified by RT-qPCR using tumor RNA from indicated mice. c,d, Prf1 and Gzmb relative expression in day 18 B16 melanoma tumors from B6.SJL mice treated with in vitro-differentiated control, Cbx3/HP1g- or Cbx3-Lef1- deficient CD8+ effector T cells on day 10 after injection of B16 tumor cells. e-g, Prf1, Gzmb and Ifng relative expression in day 33 NBL tumors. h-j,

Prf1, Gzmb and Ifng relative expression in day 33 NBL tumors from B6.SJL mice treated with in vitro-differentiated control, Cbx3/HP1g- or Cbx3-Lef1-deficient CD8+ effector T cells on day 14 after injection of NBL tumor cells. Statistics: Graphpad unpaired student t-test: *p£0.05, **p£0.01, ***p£0.001, ****p£0.0001. n = 3 tumors from each mouse strain; representative of 3 experiments.

Supplementary Files

This is a list of supplementary files associated with this preprint. Click to download.

- SupplementalMaterial.pdf